Journal of Statistical Mechanics:
Theory and Experiment

PAPER

Joint distribution of multiple boundary local times and related first-passage time problems with multiple targets

Journal of Statistical Mechanics: Theory and Experiment
An IOP and SISSA journal

PAPER: Classical statistical mechanics, equilibrium and non-equilibrium

Joint distribution of multiple boundary local times and related first-passage time problems with multiple targets

Denis S Grebenkov

Laboratoire de Physique de la Matière Condensée (UMR 7643), CNRS–Ecole Polytechnique, IP Paris, 91128 Palaiseau, France
Institute for Physics and Astronomy, University of Potsdam, 14476 Potsdam-Golm, Germany
E-mail: denis.grebenkov@polytechnique.edu

Received 23 July 2020
Accepted for publication 6 September 2020
Published 26 October 2020

Online at stacks.iop.org/JSTAT/2020/103205
https://doi.org/10.1088/1742-5468/abb6e4

Abstract. We investigate the statistics of encounters of a diffusing particle with different subsets of the boundary of a confining domain. The encounters with each subset are characterized by the boundary local time on that subset. We extend a recently proposed approach to express the joint probability density of the particle position and of its multiple boundary local times via a multi-dimensional Laplace transform of the conventional propagator satisfying the diffusion equation with mixed Robin boundary conditions. In the particular cases of an interval, a circular annulus and a spherical shell, this representation can be explicitly inverted to access the statistics of two boundary local times. We provide the exact solutions and their probabilistic interpretation for the case of an interval and sketch their derivation for two other cases. We also obtain the distributions of various associated first-passage times and discuss their applications.

Keywords: Brownian motion, chemical kinetics, diffusion

J. Stat. Mech. (2020) 103205

1742-5468/20/103205+37$33.00

Contents

1. Introduction

Diffusion-controlled reactions and related stochastic processes in an Euclidean domain $\Omega \subset \mathbb{R}^d$ are typically described by the propagator (also known as the heat kernel or the Green's function), $G_q(\boldsymbol{x}, t|\boldsymbol{x}_0)$, that is the probability density of the event that a particle started from $\boldsymbol{x}_0 \in \Omega$ at time 0 has arrived in a vicinity of a point $\boldsymbol{x} \in \Omega$ at time t without being killed (or reacted) on the boundary $\partial\Omega$ of the domain [1–3]. For ordinary diffusion, this propagator satisfies the diffusion equation (for any starting point $\boldsymbol{x}_0 \in \Omega$),

$$\partial_t G_q(\boldsymbol{x}, t|\boldsymbol{x}_0) = D\Delta G_q(\boldsymbol{x}, t|\boldsymbol{x}_0) \quad (\boldsymbol{x} \in \Omega), \tag{1}$$

J. Stat. Mech. (2020) 103205

subject to the initial condition $G_q(\boldsymbol{x}, t=0|\boldsymbol{x}_0) = \delta(\boldsymbol{x}-\boldsymbol{x}_0)$ and the Robin boundary condition on $\partial\Omega$:

$$\partial_n G_q(\boldsymbol{x}, t|\boldsymbol{x}_0) + q G_q(\boldsymbol{x}, t|\boldsymbol{x}_0) = 0 \quad (\boldsymbol{x} \in \partial\Omega), \tag{2}$$

where D is the diffusion coefficient, Δ is the Laplace operator (acting on $\boldsymbol{x}$), $\delta(\boldsymbol{x}-\boldsymbol{x}_0)$ is the Dirac distribution, and ∂_n is the normal derivative on the boundary $\partial\Omega$, oriented outward the domain Ω. The parameter q characterizes the reactivity of the boundary and ranges from $q=0$ (an inert reflecting boundary with Neumann condition) to $+\infty$ (a perfectly reactive boundary with Dirichlet condition). The intermediate case of $0 < q < +\infty$ corresponds to partial reactivity of the boundary which can represent overpassing a reaction activation barrier [4–10], the coarse-graining effect of microscopic spatial heterogeneities of reactive patches [11–22], stochastic activity of the target (open/closed channels, switching between conformational states of a macromolecule) [23–26], and other microscopic mechanisms [27–34] (see an overview in [35]). The propagator determines most commonly employed characteristics of diffusion–reaction processes such as the survival probability, the reaction time distribution, and the reaction rate, that found numerous applications in physics, chemistry and biology [36–45]. Importantly, the propagator and all related quantities depend on q *implicitly* (as a parameter of the boundary condition) that makes the study of this dependence and its eventual optimization challenging.

To overcome this limitation, we proposed an alternative description of partial reactivity in terms of the boundary local time that quantifies the encounters of a diffusing particle with the boundary of a confining domain [46]. The boundary local time ℓ_t naturally appears in the stochastic differential equation for reflected Brownian motion $\boldsymbol{X}_t$ [47–49] and can be expressed in terms of the residence time of $\boldsymbol{X}_t$ in a thin boundary layer $\partial\Omega_a$

$$\ell_t = \lim_{a\to 0} \frac{D}{a} \underbrace{\int_0^t \mathrm{d}t'\, \Theta(a - |\partial\Omega - \boldsymbol{X}_{t'}|)}_{\text{residence time in } \partial\Omega_a}, \tag{3}$$

where $\Theta(z)$ is the Heaviside step function, which represents the indicator function of a thin layer of width a near $\partial\Omega$: $\partial\Omega_a = \{\boldsymbol{x} \in \Omega : |\boldsymbol{x} - \partial\Omega| < a\}$. Note that the prefactor D/a renders ℓ_t to be in units of length. We also stress that the boundary local time should not be confused with the point local time, which was thoroughly studied in the past (see [50–52] and references therein). For reflected Brownian motion on the half-line, the distribution of the boundary local time has been studied long ago [47, 50]. In a recent paper, we proposed a general spectral approach to obtain the distribution of the boundary local time for Euclidean domains with smooth boundary by using the Dirichlet-to-Neumann operator [53]. This approach was further extended in [46] to get the joint probability density $P(\boldsymbol{x}, \ell, t|\boldsymbol{x}_0)$ of the position $\boldsymbol{X}_t$ of the particle diffusing in a domain Ω with *reflecting* boundary, and of its boundary local time ℓ_t at time t, given that it has started from a point $\boldsymbol{x}_0$ at time 0. This so-called full propagator was shown to be related to the conventional propagator $G_q(\boldsymbol{x}, t|\boldsymbol{x}_0)$ via

J. Stat. Mech. (2020) 103205

the Laplace transform:

$$G_q(\boldsymbol{x}, t|\boldsymbol{x}_0) = \int_0^\infty \mathrm{d}\ell\, \mathrm{e}^{-q\ell}\, P(\boldsymbol{x}, \ell, t|\boldsymbol{x}_0). \tag{4}$$

Here, the surface reactivity parameter q appears explicitly in the prefactor $\mathrm{e}^{-q\ell}$ which comes from the assumption of constant boundary reactivity. Other reaction mechanisms with encounter-dependent reactivity were introduced and studied in [46] (see also section 5 below). We emphasize that the propagators $G_q(\boldsymbol{x}, t|\boldsymbol{x}_0)$ (with $q > 0$) and $G_0(\boldsymbol{x}, t|\boldsymbol{x}_0)$ (or its extension $P(\boldsymbol{x}, \ell, t|\boldsymbol{x}_0)$) correspond to the distinct cases of reactive and reflecting (inert) boundaries, respectively. As the particle may react and thus disappear in the former case, the associated diffusive processes are usually distinguished in the literature. However, as argued in [46] (see also [32, 33, 35] and references therein), the diffusive process in the presence of a reactive boundary is just reflected Brownian motion in a domain with reflecting boundary, which is stopped at an appropriate random time. This property is reflected by equation (4), in which the full propagator $P(\boldsymbol{x}, \ell, t|\boldsymbol{x}_0)$ characterizes reflected Brownian motion and the prefactor $\mathrm{e}^{-q\ell}$ incorporates the stopping condition (see section 2 below for details and extensions).

In many chemical and biological applications, the reactive boundary is not homogeneous, while a reactive patch or a target is not unique. For instance, many traps can compete for capturing the diffusing particle, and one is interested in knowing the capture time for a given trap in the presence of its competitors [54]. Even a single trap can be surrounded by inert obstacles or by a reflecting boundary. When considering an escape problem, the escape region is usually a subset of the reflecting boundary. In all these situations, setting the homogeneous Robin boundary condition (2) on the whole boundary is not appropriate, as one has to distinguish surface mechanisms on different regions of the boundary. For this purpose, a spectral approach with a space-dependent reactivity was developed [55].

In this paper, we propose a complementary approach and bring some probabilistic insights onto this problem when the reactivity is piecewise constant. In this case, one can consider different reactivity regions by partitioning the boundary $\partial\Omega$ into m non-overlapping subsets Γ_i:

$$\partial\Omega = \bigcup_{i=1}^{m} \overline{\Gamma}_i, \quad \Gamma_i \cap \Gamma_j = \emptyset. \tag{5}$$

In order to characterize the encounters with different parts Γ_i of the boundary, we introduce the associated boundary local times ℓ_t^i:

$$\ell_t^i = \lim_{a\to 0} \frac{D}{a} \int_0^t \mathrm{d}t'\, \Theta(a - |\Gamma_i - \boldsymbol{X}_{t'}|) \quad (i = 1, \ldots, m). \tag{6}$$

If the joint distribution of the boundary local times ℓ_t^i was known, one could investigate various encounter properties such as 'How many times the particle has arrived on a given partially reactive trap before being absorbed by its competitors?', 'What is the first moment when the particle has visited each trap a given number of times?', etc.

J. Stat. Mech. (2020) 103205

In other words, the joint distribution of the boundary local times will provide conceptually new insights onto diffusion-controlled reactions, far beyond the conventional first-passage times (FPTs). To our knowledge, such joint distributions were not studied earlier.

In this paper, we aim at obtaining the joint distribution by extending the probabilistic arguments from [46]. In section 2, we generalize equation (4) to a multi-dimensional Laplace transform and discuss some of its properties. However, the numerical inversion of the multi-dimensional Laplace transform is challenging. For this reason, we restrict our attention to three basic domains (an interval, a circular annulus and a spherical shell) for which the inversion can be performed explicitly (section 3). In fact, we derive an exact formula for the joint probability density for the case of an interval, and discuss its straightforward extension for two other domains. We illustrate the properties of the two boundary local times and their correlations. Section 4 is devoted to various FPT problems. We first recall the basic FPTs to perfectly and partially reactive boundary and then derive the probability density of the first time when two boundary local times exceed prescribed thresholds. In other words, we fully characterize the first moment when both subsets of the boundary have been visited a prescribed number of times. In section 5, we discuss some further extensions and consequences of the obtained results for diffusion-controlled reactions.

2. General solution

The joint distribution can be derived by extending the probabilistic arguments from [46]. For this purpose, let us introduce the propagator $G_{q_1,\ldots,q_m}(\boldsymbol{x},t|\boldsymbol{x}_0)$ satisfying the diffusion equation (1) with mixed Robin boundary conditions:

$$\partial_n G_{q_1,\ldots,q_m}(\boldsymbol{x},t|\boldsymbol{x}_0) + q_i G_{q_1,\ldots,q_m}(\boldsymbol{x},t|\boldsymbol{x}_0) = 0 \quad (\boldsymbol{x}\in\Gamma_i), \tag{7}$$

with nonnegative parameters $q_1,\ldots,q_m$ characterizing each reactive part Γ_i of the boundary. In other words, we extend the constant reactivity parameter q from equation (2) by a piecewise constant function taking the values $q_1,\ldots,q_m$ on different subsets Γ_i of the boundary. As discussed in [33, 35, 56, 57], the Robin boundary condition describes partial reactivity of the boundary: the diffusing particle hitting the boundary can either react, or be reflected. To define properly the reaction probability Π at each encounter, one can introduce a thin layer of width a near the reactive part Γ_i, for which $\Pi_i = aq_i/(1+aq_i)$ (and if the particle is not reacted, it is reflected at distance a from the boundary). For a finite q_i and small a, one has $\Pi_i \approx aq_i$. In the limit $a\to 0$, the probability of the reaction event goes to 0 but the number of returns to the boundary goes to infinity, yielding a nontrivial limit. If all attempts to react are independent, the probability of not reacting on the boundary up to time t is

$$\mathcal{P}_t = \mathbb{E}_{\boldsymbol{x}_0}\left\{\prod_{i=1}^m (1-\Pi_i)^{\mathcal{N}^i_{t,a}}\right\}, \tag{8}$$

J. Stat. Mech. (2020) 103205

where $\mathcal{N}_{t,a}^i$ is the number of encounters with a thin layer near Γ_i up to time t, and $\mathbb{E}_{\boldsymbol{x}_0}$ denotes the expectation with respect to the probability measure associated with reflected Brownian motion in Ω, started from $\boldsymbol{x}_0$. In the limit $a \to 0$, this number is related to the boundary local time: $\mathcal{N}_{t,a}^i \approx \ell_t^i/a$ [47–49] so that

$$\mathcal{P}_t \approx \mathbb{E}_{\boldsymbol{x}_0}\left\{\exp\left(-\sum_{i=1}^m \Pi_i \mathcal{N}_{t,a}^i\right)\right\} \underset{a\to 0}{\to} \mathbb{E}_{\boldsymbol{x}_0}\left\{\exp\left(-\sum_{i=1}^m q_i \ell_t^i\right)\right\}. \tag{9}$$

Adding the constraint for the arrival position of the particle to be in a vicinity of $\boldsymbol{x}$, one gets the probabilistic meaning of the conventional propagator, i.e. the probability density of finding the survived particle in a vicinity of $\boldsymbol{x}$:

$$G_{q_1,\ldots,q_m}(\boldsymbol{x},t|\boldsymbol{x}_0) = \mathbb{E}_{\boldsymbol{x}_0}\left\{\exp\left(-\sum_{i=1}^m q_i \ell_t^i\right)\delta(\boldsymbol{X}_t - \boldsymbol{x})\right\}. \tag{10}$$

If $P(\boldsymbol{x},\ell_1,\ldots,\ell_m,t|\boldsymbol{x}_0)$ is the joint probability density of the position $\boldsymbol{X}_t$ and of all boundary local times ℓ_t^i, the above expectation reads

$$G_{q_1,\ldots,q_m}(\boldsymbol{x},t|\boldsymbol{x}_0) = \int_0^\infty \mathrm{d}\ell_1\, \mathrm{e}^{-q_1\ell_1}\ldots\int_0^\infty \mathrm{d}\ell_m\, \mathrm{e}^{-q_m\ell_m}\, P(\boldsymbol{x},\ell_1,\ldots,\ell_m,t|\boldsymbol{x}_0). \tag{11}$$

This is the extension of equation (4) derived in [46]. Formally, the joint probability density of the boundary local times $\ell_t^1,\ldots,\ell_t^m$ and of the position $\boldsymbol{X}_t$ can be obtained from the propagator $G_{q_1,\ldots,q_m}(\boldsymbol{x},t|\boldsymbol{x}_0)$ by performing the m-fold Laplace transform inversion.

The (marginal) joint probability density of the boundary local times $\ell_t^1,\ldots,\ell_t^m$ is simply

$$P(\circ,\ell_1,\ldots,\ell_m,t|\boldsymbol{x}_0) = \int_\Omega \mathrm{d}\boldsymbol{x}\, P(\boldsymbol{x},\ell_1,\ldots,\ell_m,t|\boldsymbol{x}_0) \tag{12}$$

(we use the notation $\circ$ for marginalized variables). Integrating equation (11) over $\boldsymbol{x}\in\Omega$, one gets

$$S_{q_1,\ldots,q_m}(t|\boldsymbol{x}_0) = \int_0^\infty \mathrm{d}\ell_1\, \mathrm{e}^{-q_1\ell_1}\ldots\int_0^\infty \mathrm{d}\ell_m\, \mathrm{e}^{-q_m\ell_m}\, P(\circ,\ell_1,\ldots,\ell_m,t|\boldsymbol{x}_0), \tag{13}$$

where

$$S_{q_1,\ldots,q_m}(t|\boldsymbol{x}_0) = \int_\Omega \mathrm{d}\boldsymbol{x}\, G_{q_1,\ldots,q_m}(\boldsymbol{x},t|\boldsymbol{x}_0) \tag{14}$$

is the survival probability up to time t in the presence of reactive traps, which obeys the backward diffusion equation:

$$\partial_t S_{q_1,\ldots,q_m}(t|\boldsymbol{x}_0) = D\Delta S_{q_1,\ldots,q_m}(t|\boldsymbol{x}_0) \quad (\boldsymbol{x}_0\in\Omega), \tag{15}$$

$$\partial_n S_{q_1,\ldots,q_m}(t|\boldsymbol{x}_0) + q_i S_{q_1,\ldots,q_m}(t|\boldsymbol{x}_0) = 0 \quad (\boldsymbol{x}_0\in\Gamma_i), \tag{16}$$

J. Stat. Mech. (2020) 103205

subject to the initial (terminal) condition $S_{q_1,\ldots,q_m}(t=0|\boldsymbol{x}_0)=1$. Note also that the Laplace transform (13) allows one to determine joint positive-order integer moments of the boundary local times:

$$\mathbb{E}_{\boldsymbol{x}_0}\left\{[\ell_t^1]^{k_1}\ldots[\ell_t^m]^{k_m}\right\}=(-1)^{k_1+\cdots+k_m}\lim_{q_1,\ldots,q_m\to 0}\frac{\partial^{k_1+\cdots+k_m}}{\partial q_1^{k_1}\ldots\partial q_m^{k_m}}S_{q_1,\ldots,q_m}(t|\boldsymbol{x}_0) \tag{17}$$

for any integer $k_1,\ldots,k_m\geqslant 0$ (in turn, using equation (11), one gets the moments under the additional constraint of being in $\boldsymbol{x}$ at time t).

As reflected Brownian motion is a Markovian process, the conventional propagator $G_{q_1,\ldots,q_m}(\boldsymbol{x},t|\boldsymbol{x}_0)$ gives access to the joint probability density of k positions $\boldsymbol{x}^1,\boldsymbol{x}^2,\ldots,\boldsymbol{x}^k$ at successive times $0<t_1<t_2<\ldots<t_k$ as

$$G_{q_1,\ldots,q_m}(\boldsymbol{x}^1,t_1|\boldsymbol{x}_0)\,G_{q_1,\ldots,q_m}(\boldsymbol{x}^2,t_2-t_1|\boldsymbol{x}^1)\ldots G_{q_1,\ldots,q_m}(\boldsymbol{x}^k,t_k-t_{k-1}|\boldsymbol{x}^{k-1}). \tag{18}$$

The same property holds for the full propagator, which determines the successive positions $\boldsymbol{x}^j$ and values of all boundary local times ℓ_i^j $(j=1,\ldots,k,\ i=1,\ldots,m)$ at times $t_1,t_2,\ldots,t_k$:

$$\begin{aligned}&P(\boldsymbol{x}^1,\ell_1^1,\ldots,\ell_m^1,t_1|\boldsymbol{x}_0)\,P(\boldsymbol{x}^2,\ell_1^2-\ell_1^1,\ldots,\ell_m^2-\ell_m^1,t_2-t_1|\boldsymbol{x}^1)\\&\quad\ldots P(\boldsymbol{x}^k,\ell_1^k-\ell_1^{k-1},\ldots,\ell_m^k-\ell_m^{k-1},t_k-t_{k-1}|\boldsymbol{x}^{k-1}).\end{aligned} \tag{19}$$

Even though equations (11) and (13) give access to the joint probability densities $P(\boldsymbol{x},\ell_1,\ldots,\ell_m,t|\boldsymbol{x}_0)$ and $P(\circ,\ell_1,\ldots,\ell_m,t|\boldsymbol{x}_0)$, these expressions are in general rather formal because the propagator $G_{q_1,\ldots,q_m}(\boldsymbol{x},t|\boldsymbol{x}_0)$ and the survival probability $S_{q_1,\ldots,q_m}(t|\boldsymbol{x}_0)$ are rarely known analytically, whereas the numerical inversion of the (multi-dimensional) Laplace transform can be unstable [58]. For this reason, obtaining these joint probability densities in a more constructive way (such as the spectral approach in [46]) remains an open problem.

Lacking yet a general constructive approach, we further focus on joint probability densities for three basic domains: an interval, a circular annulus between two concentric circles, and a spherical shell between two concentric spheres. The boundary of these domains naturally splits into two disjoint parts Γ_1 and Γ_2, so that we are limited to $m=2$. In two and three dimensions, the rotational symmetry of these domains reduces the computation to a one-dimensional setting for which the joint probability densities can be derived analytically. This derivation relies on the explicit form of the propagator in the Laplace domain (with respect to time t, denoted by tilde throughout the paper):

$$\tilde{G}_{q_1,q_2}(\boldsymbol{x},p|\boldsymbol{x}_0)=\int_0^\infty \mathrm{d}t\,\mathrm{e}^{-pt}\,G_{q_1,q_2}(\boldsymbol{x},t|\boldsymbol{x}_0), \tag{20}$$

which obeys the modified Helmholtz equation

$$(p-D\Delta)\tilde{G}_{q_1,q_2}(\boldsymbol{x},p|\boldsymbol{x}_0)=\delta(\boldsymbol{x}-\boldsymbol{x}_0)\quad(\boldsymbol{x}\in\Omega), \tag{21}$$

with Robin boundary conditions

$$\left(\partial_n\tilde{G}_{q_1,q_2}(\boldsymbol{x},p|\boldsymbol{x}_0)+q_i\tilde{G}_{q_1,q_2}(\boldsymbol{x},p|\boldsymbol{x}_0)\right)\Big|_{\boldsymbol{x}\in\Gamma_i}=0\quad(i=1,2). \tag{22}$$

J. Stat. Mech. (2020) 103205

Note that the Laplace-transformed propagator also allows one to describe diffusion-influenced reactions for mortal particles [59–61]. In the next section, we present the detailed derivation for an interval, while its extension to an annulus and a spherical shell will be sketched in section 3.7.

3. Exact explicit solution

For an interval $(0, b)$, the boundary consists of two endpoints, $\Gamma_1 = \{0\}$ and $\Gamma_2 = \{b\}$, and the Laplace-transformed propagator satisfying equations (21) and (22), is known explicitly [62] (see [63] for details):

$$D\tilde{G}_{q_1,q_2}(x,p|x_0) = \frac{1}{\alpha V(\alpha)} \times \begin{cases} v^b(x_0)v^0(x), & 0 \leqslant x \leqslant x_0, \\ v^0(x_0)v^b(x), & x_0 \leqslant x \leqslant b, \end{cases} \tag{23}$$

where

$$\begin{aligned} v^0(x) &= q_1 \ \sinh(\alpha x) + \alpha \ \cosh(\alpha x), \\ v^b(x) &= q_2 \ \sinh(\alpha(b-x)) + \alpha \ \cosh(\alpha(b-x)), \\ V &= (\alpha^2 + q_1 q_2)\sinh(\alpha b) + \alpha(q_1+q_2)\cosh(\alpha b), \end{aligned}$$

with $\alpha = \sqrt{p/D}$. We aim at evaluating explicitly the inverse double Laplace transform with respect to q_1 and q_2 (denoted as $\mathcal{L}_2^{-1}$) to get the full propagator:

$$\tilde{P}(x,\ell_1,\ell_2,p|x_0) = \mathcal{L}_2^{-1}\left\{\tilde{G}_{q_1,q_2}(x,p|x_0)\right\}, \tag{24}$$

i.e. the Laplace transform (with respect to time t) of the joint probability density of the position x and two boundary local times ℓ_1 and ℓ_2 at endpoints Γ_1 and Γ_2, respectively. Even though an extra Laplace inversion will be needed to get $P(x,\ell_1,\ell_2,t|x_0)$ in time domain, this is much simpler than the original double Laplace transform. Moreover, it is common to operate with diffusion characteristics in the Laplace domain, in particular, when studying FPTs (see below).

3.1. Moments of the boundary local times

Before deriving the full propagator, we start by looking at the positive moments of two boundary local times:

$$M_{k_1,k_2}(t) = \mathbb{E}_{x_0}\left\{[\ell_t^1]^{k_1}\,[\ell_t^2]^{k_2}\right\}. \tag{25}$$

According to equation (17), the Laplace transform of these moments can be obtained by integrating the propagator $\tilde{G}_{q_1,q_2}(x,p|x_0)$ over x and differentiating with respect to q_1 and q_2:

$$\tilde{M}_{k_1,k_2}(p) = (-1)^{k_1+k_2}\lim_{q_1,q_2\to 0}\frac{\partial^{k_1+k_2}}{\partial q_1^{k_1}\partial q_2^{k_2}}\tilde{S}_{q_1,q_2}(p|x_0), \tag{26}$$

J. Stat. Mech. (2020) 103205

where

$$\tilde{S}_{q_1,q_2}(x,p|x_0) = \int_0^b \mathrm{d}x\, \tilde{G}_{q_1,q_2}(x,p|x_0) = \frac{1}{D\alpha^2 V(\alpha)} \times \left\{ q_1 q_2 \left(\sinh(\alpha b) - \sinh(\alpha(b-x_0)) - \sinh(\alpha x_0)\right) + \alpha^2 \sinh(\alpha b) + \alpha q_1 \left(\cosh(\alpha b) - \cosh(\alpha(b-x_0))\right) + \alpha q_2 \left(\cosh(\alpha b) - \cosh(\alpha x_0)\right) \right\}. \tag{27}$$

For instance, one gets the Laplace transform of the mean values,

$$\tilde{M}_{1,0}(p) = \frac{\cosh(\alpha(b-x_0))}{D\alpha^3 \sinh(\alpha b)}, \qquad \tilde{M}_{0,1}(p) = \frac{\cosh(\alpha x_0)}{D\alpha^3 \sinh(\alpha b)}, \tag{28}$$

second moments,

$$\tilde{M}_{2,0}(p) = \frac{2\cosh(\alpha b)\cosh(\alpha(b-x_0))}{D\alpha^4 \sinh^2(\alpha b)}, \qquad \tilde{M}_{0,2}(p) = \frac{2\cosh(\alpha b)\cosh(\alpha x_0)}{D\alpha^4 \sinh^2(\alpha b)}, \tag{29}$$

and the cross-moment

$$\tilde{M}_{1,1}(p) = \frac{\sinh(\alpha x_0) + \sinh(\alpha(b-x_0))}{D\alpha^4 \sinh(\alpha b)(\cosh(\alpha b) - 1)}. \tag{30}$$

Even so the inverse Laplace transform of these moments can be computed exactly by the residue theorem, we just provide the asymptotic behavior of the mean values:

- At short times,

$$\mathbb{E}_{x_0}\left\{\ell_t^1\right\} \simeq \begin{cases} \dfrac{4(Dt)^{3/2}\, \mathrm{e}^{-x_0^2/(4Dt)}}{\sqrt{\pi} x_0^2} & (x_0 > 0), \\ \dfrac{2\sqrt{Dt}}{\sqrt{\pi}} & (x_0 = 0), \end{cases} \tag{31}$$

$$\mathbb{E}_{x_0}\left\{\ell_t^2\right\} \simeq \begin{cases} \dfrac{4(Dt)^{3/2}\, \mathrm{e}^{-(b-x_0)^2/(4Dt)}}{\sqrt{\pi}(b-x_0)^2} & (x_0 < b), \\ \dfrac{2\sqrt{Dt}}{\sqrt{\pi}} & (x_0 = b)\,; \end{cases} \tag{32}$$

- At long times

$$\mathbb{E}_{x_0}\left\{\ell_t^1\right\} \simeq \frac{Dt}{b} + \frac{2b^2 - 6bx_0 + 3x_0^2}{6b}, \qquad \mathbb{E}_{x_0}\left\{\ell_t^2\right\} \simeq \frac{Dt}{b} + \frac{3x_0^2 - b^2}{6b}. \tag{33}$$

Performing the same analysis for the second moment, we get the long-time behavior of the variance, which does not depend on x_0 and b in the leading order:

$$\mathrm{var}\left\{\ell_t^1\right\} \simeq \mathrm{var}\left\{\ell_t^2\right\} \simeq 2Dt + O(1) \quad (t \to \infty). \tag{34}$$

Finally, we get

$$M_{1,1} \simeq -Dt/3 + O(1) \quad (t \to \infty), \tag{35}$$

J. Stat. Mech. (2020) 103205

so that the correlation between two boundary local times approaches $-1/6$ at long times. As expected, the correlation is negative: when ℓ_t^1 is larger than its mean, the particle spent more time on the endpoint Γ_1, and thus ℓ_t^2 is expected to be smaller than its mean.

3.2. Derivation of the full propagator

Let us focus on the case $0 \leqslant x \leqslant x_0$ and write explicitly

$$D\tilde{G}_{q_1,q_2}(x,p|x_0) = Q(q_1,q_2)\frac{\sinh(\alpha(b-x_0))\sinh(\alpha x)}{\alpha\ \sinh(\alpha b)}, \tag{36}$$

where

$$Q(q_1,q_2) = \frac{[q_2+\alpha\,\mathrm{ctanh}(\alpha(b-x_0))][q_1+\alpha\,\mathrm{ctanh}(\alpha x)]}{q_1q_2+\alpha(q_1+q_2)\mathrm{ctanh}(\alpha b)+\alpha^2}. \tag{37}$$

To invert this double Laplace transform, we use the following properties [65]:

$$\mathcal{L}_2\{\mathrm{e}^{-k_1\ell_1-k_2\ell_2}\,f(\ell_1,\ell_2)\} = \mathcal{L}_2\{f\}(q_1+k_1,q_2+k_2), \tag{38}$$

$$\mathcal{L}_2\{I_0(a\sqrt{\ell_1\ell_2})\} = \frac{1}{q_1q_2-a^2/4}, \tag{39}$$

$$\mathcal{L}_2\{\partial_{\ell_1}f(\ell_1,\ell_2)\} = q_1\mathcal{L}_2\{f\}-\mathcal{L}\{f(0,\ell_2)\}, \tag{40}$$

where $\mathcal{L}$ and $\mathcal{L}_2$ denote the single and double Laplace transforms of some function f, and $I_\nu(z)$ is the modified Bessel function of the first kind.

Using the first property, one can make the change $q_1 \to \bar{q}_1 = q_1 + C$ and $q_2 \to \bar{q}_2 = q_2 + C$ with

$$C = \alpha\,\mathrm{ctanh}(\alpha b), \tag{41}$$

so that

$$Q(q_1,q_2) = \bar{Q}(\bar{q}_1,\bar{q}_2) = \frac{(\bar{q}_2+A)(\bar{q}_1+B)}{\bar{q}_1\bar{q}_2-E^2/4}, \tag{42}$$

where

$$E = 2\sqrt{C^2-\alpha^2} = 2\alpha\sqrt{\mathrm{ctanh}^2(\alpha b)-1} = \frac{2\alpha}{\sinh(\alpha b)} > 0, \tag{43}$$

$$A = \alpha\,\mathrm{ctanh}(\alpha(b-x_0))-C, \tag{44}$$

$$B = \alpha\,\mathrm{ctanh}(\alpha x)-C. \tag{45}$$

We represent the above function as

$$\bar{Q}(\bar{q}_1,\bar{q}_2) = 1 + A\frac{\bar{q}_1}{\bar{q}_1\bar{q}_2-E^2/4} + B\frac{\bar{q}_2}{\bar{q}_1\bar{q}_2-E^2/4} + (E^2/4+AB)\frac{1}{\bar{q}_1\bar{q}_2-E^2/4}. \tag{46}$$

J. Stat. Mech. (2020) 103205

The inverse double Laplace transform of the first term yields $\delta(\ell_1)\delta(\ell_2)$, whereas equation (40) allows one to compute it for the last term. Using the properties (39) and (40), we can also write

$$\mathcal{L}_2\left\{\partial_{\ell_1} I_0(a\sqrt{\ell_1\ell_2})\right\} = \mathcal{L}_2\left\{\frac{a\sqrt{\ell_2} I_1(a\sqrt{\ell_1\ell_2})}{2\sqrt{\ell_1}}\right\} = \frac{q_1}{q_1q_2 - a^2/4} - \frac{1}{q_2}, \tag{47}$$

$$\mathcal{L}_2\left\{\partial_{\ell_2} I_0(a\sqrt{\ell_1\ell_2})\right\} = \mathcal{L}_2\left\{\frac{a\sqrt{\ell_1} I_1(a\sqrt{\ell_1\ell_2})}{2\sqrt{\ell_2}}\right\} = \frac{q_2}{q_1q_2 - a^2/4} - \frac{1}{q_1}. \tag{48}$$

These relations allow us to invert the second and third terms in equation (46). Combining these results, we get

$$\begin{aligned}\mathcal{L}_2^{-1}\{\bar{Q}\} = \delta(\ell_1)\delta(\ell_2) &+ A\left(\frac{E\sqrt{\ell_2} I_1(E\sqrt{\ell_1\ell_2})}{2\sqrt{\ell_1}} + \delta(\ell_1)\right)\\ &+ B\left(\frac{E\sqrt{\ell_1} I_1(E\sqrt{\ell_1\ell_2})}{2\sqrt{\ell_2}} + \delta(\ell_2)\right) + (E^2/4 + AB) I_0\left(E\sqrt{\ell_1\ell_2}\right),\end{aligned}$$

from which the full propagator reads (for $0 \leqslant x \leqslant x_0 \leqslant b$):

$$D\tilde{P}(x, \ell_1, \ell_2, p|x_0) = \frac{\sinh(\alpha(b - x_0))\sinh(\alpha x)}{\alpha\ \sinh(\alpha b)} \mathrm{e}^{-C(\ell_1+\ell_2)} \mathcal{L}_2^{-1}\{\bar{Q}\}. \tag{49}$$

After simplifications, this relation becomes

$$\begin{aligned}\tilde{P}(x, \ell_1, \ell_2, p|x_0) = &\underbrace{\frac{\sinh(\alpha(b - x_0))\sinh(\alpha x)}{D\alpha\ \sinh(\alpha b)}}_{=\tilde{G}_{\infty,\infty}(x,p|x_0)} \delta(\ell_1)\delta(\ell_2) + \underbrace{\frac{\sinh(\alpha x)}{\sinh(\alpha b)}}_{=\tilde{j}_{\infty,\infty}(b,p|x)} \delta(\ell_1)\frac{\mathrm{e}^{-C\ell_2}}{D}\underbrace{\frac{\sinh(\alpha x_0)}{\sinh(\alpha b)}}_{=\tilde{j}_{\infty,\infty}(b,p|x_0)}\\ &+ \underbrace{\frac{\sinh(\alpha(b - x))}{\sinh(\alpha b)}}_{=\tilde{j}_{\infty,\infty}(0,p|x)} \delta(\ell_2)\frac{\mathrm{e}^{-C\ell_1}}{D}\underbrace{\frac{\sinh(\alpha(b - x_0))}{\sinh(\alpha b)}}_{=\tilde{j}_{\infty,\infty}(0,p|x_0)} + \left\{\frac{\sinh(\alpha x)\sinh(\alpha x_0)}{\sinh^2(\alpha b)}\right.\\ &\times \frac{\sqrt{\ell_2} I_1(E\sqrt{\ell_1\ell_2})}{\sqrt{\ell_1}} + \frac{\sinh(\alpha(b - x))\sinh(\alpha(b - x_0))}{\sinh^2(\alpha b)}\frac{\sqrt{\ell_1} I_1(E\sqrt{\ell_1\ell_2})}{\sqrt{\ell_2}}\\ &\left.+ \frac{\sinh(\alpha x_0)\sinh(\alpha(b - x)) + \sinh(\alpha x)\sinh(\alpha(b - x_0))}{\sinh^2(\alpha b)} I_0(E\sqrt{\ell_1\ell_2})\right\}\\ &\times \frac{E}{2D}\mathrm{e}^{-C(\ell_1+\ell_2)}.\end{aligned} \tag{50}$$

In the opposite case $0 \leqslant x_0 \leqslant x \leqslant b$, one exchanges x_0 and x. This is one of the main explicit results of the paper.

3.3. Probabilistic interpretation

Let us discuss the structure of the derived full propagator in equation (50). The first term represents the contributions of 'direct' trajectories from x_0 to x that do not hit

J. Stat. Mech. (2020) 103205

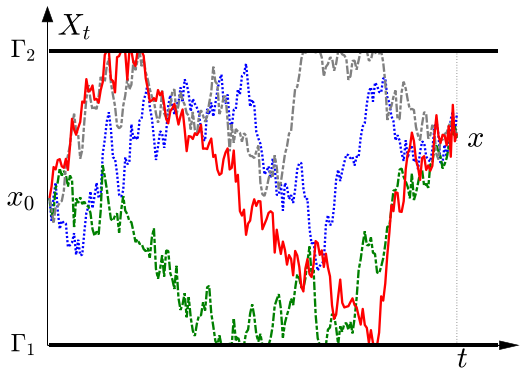

Figure 1. Four simulated trajectories on the interval $(0, b)$, each started from x_0 at time 0 and arrived to x at time t: a direct trajectory that does not hit either of the endpoints (blue dotted line); a trajectory that does not hit the upper endpoint $\Gamma_2 = \{b\}$ (green dashed line); a trajectory that does not hit the bottom endpoint $\Gamma_1 = \{0\}$ (gray dashed line); a trajectory that hits both endpoints (red solid line).

either of the endpoints (figure 1). As a consequence, the boundary local times ℓ_1 and ℓ_2 remain zero, as represented by Dirac distributions $\delta(\ell_1)\delta(\ell_2)$. The factor in front of these distributions is the propagator $\tilde{G}_{\infty,\infty}(x, p|x_0)$ for an interval $(0, b)$ with absorbing endpoints (i.e. with Dirichlet boundary conditions that correspond to $q_1 = q_2 = \infty$). This propagator represents the fraction of direct trajectories from x_0 to x.

In the same vein, the second term represents the contribution of trajectories that do not hit the left endpoint Γ_1 but may repeatedly hit the right endpoint Γ_2. Introducing the Laplace-transformed probability flux densities,

$$\tilde{j}_{\infty,\infty}(0, p|x_0) = \left(-D\partial_n \tilde{G}_{\infty,\infty}(x, p|x_0)\right)\Big|_{x=0} = \frac{\sinh(\alpha(b - x_0))}{\sinh(\alpha b)}, \tag{51}$$

$$\tilde{j}_{\infty,\infty}(b, p|x_0) = \left(-D\partial_n \tilde{G}_{\infty,\infty}(x, p|x_0)\right)\Big|_{x=b} = \frac{\sinh(\alpha x_0)}{\sinh(\alpha b)}, \tag{52}$$

the factor in front of $\delta(\ell_1)$ reads as

$$\tilde{j}_{\infty,\infty}(b, p|x_0)\,\frac{\mathrm{e}^{-C\ell_2}}{D}\,\tilde{j}_{\infty,\infty}(b, p|x).$$

This factor has a clear probabilistic interpretation: the first arrival from x_0 to $\Gamma_2 = \{b\}$, multiple reflections on that boundary that increases its boundary local time ℓ_2 but *conditioned to avoid hitting* Γ_1, and the last direct move from Γ_2 to x. As the computations are performed in Laplace domain (with respect to time t), the product of these three factors corresponds to the convolution in time domain, as expected. The contribution of such multiple returns to Γ_2 is given by $\mathrm{e}^{-C\ell_2}/D$, where $C = \alpha\mathrm{ctanh}(\alpha b)$ can be interpreted as the eigenvalue of the Dirichlet-to-Neumann operator on the interval $(0, b)$ with the condition of avoiding Γ_1 (see appendix A).

J. Stat. Mech. (2020) 103205

Similarly, the third term with $\delta(\ell_2)$ accounts for the trajectories that do not hit the right endpoint Γ_2 but may repeatedly hit the left one Γ_1. The remaining terms in equation (50) give the contribution of all other trajectories that hit both endpoints.

3.4. Marginal probability quantities

By integrating the full propagator in equation (50) over x, we compute the marginal joint probability density of two boundary local times (in Laplace domain with respect to t):

$$\begin{aligned}\tilde{P}(\circ,\ell_1,\ell_2,p|x_0) = {} & \underbrace{\frac{\sinh(\alpha b)-\sinh(\alpha(b-x_0))-\sinh(\alpha x_0)}{D\alpha^2\ \sinh(\alpha b)}}_{=\tilde{S}_{\infty,\infty}(p|x_0)}\delta(\ell_1)\delta(\ell_2)\\ & + \frac{\cosh(\alpha b)-1}{\alpha\ \sinh(\alpha b)}\underbrace{\frac{\sinh(\alpha x_0)}{\sinh(\alpha b)}}_{=\tilde{j}_{\infty,\infty}(b,p|x_0)}\frac{\mathrm{e}^{-C\ell_2}}{D}\,\delta(\ell_1) + \frac{\cosh(\alpha b)-1}{\alpha\ \sinh(\alpha b)}\underbrace{\frac{\sinh(\alpha(b-x_0))}{\sinh(\alpha b)}}_{=\tilde{j}_{\infty,\infty}(0,p|x_0)}\\ & \times\frac{\mathrm{e}^{-C\ell_1}}{D}\,\delta(\ell_2) + \frac{\cosh(\alpha b)-1}{\alpha\ \sinh(\alpha b)}\left(\frac{\sinh(\alpha x_0)}{\sinh(\alpha b)}\frac{\sqrt{\ell_2}I_1(E\sqrt{\ell_1\ell_2})}{\sqrt{\ell_1}} + \frac{\sinh(\alpha(b-x_0))}{\sinh(\alpha b)}\right.\\ & \left.\times\frac{\sqrt{\ell_1}I_1(E\sqrt{\ell_1\ell_2})}{\sqrt{\ell_2}} + \frac{\sinh(\alpha x_0)+\sinh(\alpha(b-x_0))}{\sinh(\alpha b)}I_0(E\sqrt{\ell_1\ell_2})\right)\frac{E}{2D}\mathrm{e}^{-C(\ell_1+\ell_2)}.\end{aligned} \tag{53}$$

Its probabilistic interpretation is similar to that of the full propagator.

In turn, the integral of $\tilde{P}(x,\ell_1,\ell_2,p|x_0)$ over ℓ_2 yields the marginal joint probability density of x and ℓ_1 (for $0\leqslant x\leqslant x_0\leqslant b$):

$$\begin{aligned}\tilde{P}(x,\ell_1,\circ,p|x_0) = {} & \delta(\ell_1)\underbrace{\frac{\sinh(\alpha x)\cosh(\alpha(b-x_0))}{D\alpha\ \cosh(\alpha b)}}_{=\tilde{G}_{\infty,0}(x,p|x_0)}\\ & + \frac{\mathrm{e}^{-\alpha\ \tanh(\alpha b)\ell_1}}{D}\underbrace{\frac{\cosh(\alpha(b-x_0))}{\cosh(\alpha b)}}_{=\tilde{j}_{\infty,0}(0,p|x_0)}\underbrace{\frac{\cosh(\alpha(b-x))}{\cosh(\alpha b)}}_{=\tilde{j}_{\infty,0}(0,p|x)}\end{aligned} \tag{54}$$

(x and x_0 should be exchanged when $x>x_0$). Expectedly, the term in front of $\delta(\ell_1)$ is the propagator $\tilde{G}_{\infty,0}(x,p|x_0)$ for an interval $(0,b)$ with Dirichlet condition at $x=0$ and Neumann condition at $x=b$. In fact, as one is not interested anymore in the boundary local time ℓ_2 here, one can put the Neumann boundary condition at $x=b$. In the factor $\alpha\tanh(\alpha b)$, one can recognize the eigenvalue of the Dirichlet-to-Neumann operator on that interval that corresponds to the eigenfunction $v=1$ (see appendix A). Finally, the factor $\cosh(\alpha(b-x_0))/\cosh(\alpha b)$ is simply the Laplace-transformed probability flux density $\tilde{j}_{\infty,0}(0,p|x_0)$.

J. Stat. Mech. (2020) 103205

Integrating equation (54) over x, one gets the marginal probability density of the boundary local time ℓ_1:

$$\tilde{P}(\circ,\ell_1,\circ,p|x_0)=\delta(\ell_1)\underbrace{\frac{\cosh(\alpha b)-\cosh(\alpha(b-x_0))}{D\alpha^2\ \cosh(\alpha b)}}_{=\tilde{S}_{\infty,0}(p|x_0)} + \frac{\mathrm{e}^{-\alpha\ \tanh(\alpha b)\ell_1}}{D}\underbrace{\frac{\cosh(\alpha(b-x_0))}{\cosh(\alpha b)}}_{=\tilde{j}_{\infty,0}(0,p|x_0)}\frac{\sinh(\alpha b)}{\alpha\ \cosh(\alpha b)}. \tag{55}$$

Similarly, the marginal probability density of the boundary local time ℓ_2 is

$$\tilde{P}(\circ,\circ,\ell_2,p|x_0)=\delta(\ell_2)\underbrace{\frac{\cosh(\alpha b)-\cosh(\alpha x_0)}{D\alpha^2\ \cosh(\alpha b)}}_{=\tilde{S}_{0,\infty}(p|x_0)} + \frac{\mathrm{e}^{-\alpha\ \tanh(\alpha b)\ell_2}}{D}\underbrace{\frac{\cosh(\alpha x_0)}{\cosh(\alpha b)}}_{=\tilde{j}_{0,\infty}(b,p|x_0)}\frac{\sinh(\alpha b)}{\alpha\ \cosh(\alpha b)}. \tag{56}$$

Note also that the joint probability density of the position X_t and of the total boundary local time, $\ell_t=\ell_t^1+\ell_t^2$, can be obtained in the Laplace domain as

$$\begin{aligned}\int_0^\infty \mathrm{d}\ell\,\mathrm{e}^{-q\ell}\tilde{P}_{\mathrm{tot}}(x,\ell,p|x_0) &= \int_0^\infty \mathrm{d}\ell\,\mathrm{e}^{-q\ell}\int_0^\infty \mathrm{d}\ell_1\int_0^\infty \mathrm{d}\ell_2\,\delta(\ell_1+\ell_2-\ell)\,\tilde{P}(x,\ell_1,\ell_2,p|x_0)\\ &= \tilde{G}_{q,q}(x,p|x_0).\end{aligned} \tag{57}$$

One can either perform the single Laplace transform inversion of $\tilde{G}_{q,q}(x,p|x_0)$ with respect to q, or use the general spectral expansion derived in [46] based on the Dirichlet-to-Neumann operator, see equation (A.7).

Finally, in the limit $b\to\infty$, the full propagator converges to

$$\tilde{P}_{b=\infty}(x,\ell_1,\ell_2,p|x_0)=\frac{\delta(\ell_2)}{D}\left(\mathrm{e}^{-\alpha x_0}\frac{\sinh(\alpha x)}{\alpha}\delta(\ell_1)+\mathrm{e}^{-\alpha(x+x_0)}\ \mathrm{e}^{-\alpha\ell_1}\right)\quad(0\leqslant x\leqslant x_0) \tag{58}$$

(in the opposite case $x_0<x$, one exchanges x_0 and x). Expectedly, the boundary local time ℓ_2 always remains 0 (see the factor $\delta(\ell_2)$) as the right endpoint Γ_2 has moved to infinity and became unreachable. Integrating over redundant variable ℓ_2, one retrieves thus the full propagator on the half-line. Note that the inverse Laplace transform of this expression can be performed explicitly:

$$P_{b=\infty}(x,\ell_1,\circ,t|x_0)=\delta(\ell_1)\underbrace{\left(\frac{\exp\left(-\frac{(x-x_0)^2}{4Dt}\right)}{\sqrt{4\pi Dt}}-\frac{\exp\left(-\frac{(x+x_0)^2}{4Dt}\right)}{\sqrt{4\pi Dt}}\right)}_{=G_\infty(x,t|x_0)} + (x+x_0+\ell_1)\frac{\exp\left(-\frac{(x+x_0+\ell_1)^2}{4Dt}\right)}{\sqrt{4\pi D^3t^3}}. \tag{59}$$

J. Stat. Mech. (2020) 103205

In turn, the integral of equation (58) over x yields the marginal probability density of ℓ_1:

$$\tilde{P}_{b=\infty}(\circ,\ell_1,\circ,p|x_0)=\frac{1-\mathrm{e}^{-\alpha x_0}}{D\alpha^2}\delta(\ell_1)+\frac{\mathrm{e}^{-\alpha x_0}}{D\alpha}\mathrm{e}^{-\alpha\ell_1}\quad(x_0\geqslant 0),\tag{60}$$

which can also be inverted:

$$P_{b=\infty}(\circ,\ell_1,\circ,t|x_0)=\operatorname{erf}\left(\frac{x_0}{\sqrt{4Dt}}\right)\delta(\ell_1)+\frac{\exp\left(-\frac{(x_0+\ell_1)^2}{4Dt}\right)}{\sqrt{\pi Dt}}\quad(x_0\geqslant 0),\tag{61}$$

in agreement with [63].

3.5. Joint cumulative probability function

The statistics of two boundary local times ℓ_t^1 and ℓ_t^2 is fully determined by the marginal joint probability density $P(\circ,\ell_1,\ell_2,t|x_0)$. For some applications (see below), it is more convenient to deal with the joint cumulative probability function:

$$F(\ell_1,\ell_2,t|x_0)=\int_0^{\ell_1}\mathrm{d}\ell_1'\int_0^{\ell_2}\mathrm{d}\ell_2'\,P(\circ,\ell_1',\ell_2',t|x_0).\tag{62}$$

Using equation (53), we obtain after simplifications

$$\begin{aligned}\tilde{F}(\ell_1,\ell_2,p|x_0)=\tilde{S}_{\infty,\infty}(p|x_0)&+\frac{\sinh(\alpha x_0)+\sinh(\alpha(b-x_0))}{D\alpha^2\ \sinh(\alpha b)}Q_2\left(C\ell_1,C\ell_2\,;\operatorname{sech}(\alpha b)\right)\\&+\frac{(\cosh(\alpha b)-1)\sinh(\alpha x_0)}{D\alpha^2\ \cosh(\alpha b)\sinh(\alpha b)}\mathrm{e}^{-\alpha\,\tanh(\alpha b)\ell_1}Q_1\left(C\ell_2\,;\sqrt{C\ell_1}\operatorname{sech}(\alpha b)\right)\\&+\frac{(\cosh(\alpha b)-1)\sinh(\alpha(b-x_0))}{D\alpha^2\ \cosh(\alpha b)\sinh(\alpha b)}\mathrm{e}^{-\alpha\,\tanh(\alpha b)\ell_2}Q_1\left(C\ell_1\,;\sqrt{C\ell_2}\operatorname{sech}(\alpha b)\right),\end{aligned}\tag{63}$$

where $\operatorname{sech}(z)=1/\cosh(z)$,

$$\tilde{S}_{\infty,\infty}(p|x_0)=\frac{\sinh(\alpha b)-\sinh(\alpha(b-x_0))-\sinh(\alpha x_0)}{D\alpha^2\ \sinh(\alpha b)},\tag{64}$$

and we introduced two auxiliary functions:

$$Q_1(z\,;a)=\mathrm{e}^{-a^2}\int_0^z\mathrm{d}x\,\mathrm{e}^{-x}\,I_0(2a\sqrt{x}),\tag{65}$$

$$Q_2(z_1,z_2\,;a)=(1-a^2)\int_0^{z_1}\mathrm{d}x_1\int_0^{z_2}\mathrm{d}x_2\,\mathrm{e}^{-x_1-x_2}\,I_0(2a\sqrt{x_1x_2}).\tag{66}$$

Strictly speaking, the first term in equation (63) should include the Heaviside functions $\Theta(\ell_1)\Theta(\ell_2)$, which after differentiation with respect to ℓ_1 and ℓ_2 yields $\delta(\ell_1)\delta(\ell_2)$ in the first term in equation (50). Similarly, some other terms should include $\Theta(\ell_1)$ and $\Theta(\ell_2)$ but we omit them for brevity by considering $\ell_1>0$ and $\ell_2>0$. Setting $\ell_1=\ell_2=0$, one retrieves the Laplace-transformed survival probability $\tilde{S}_{\infty,\infty}(p|x_0)$, as expected.

J. Stat. Mech. (2020) 103205

The definition of the functions Q_1 and Q_2 ensures that $Q_1(\infty\,;a)=1$ and $Q_2(\infty,\infty\,;a)=1$ so that $\tilde{F}(\infty,\infty,p|x_0)=1/p$ and thus $F(\infty,\infty,t|x_0)=1$ as expected. Moreover, since $Q_1(z\,;\infty)=0$ and $Q_2(\infty,z\,;a)=1-\mathrm{e}^{-z(1-a^2)}$, one easily finds the Laplace transforms of the marginal cumulative probability functions:

$$\tilde{F}(\ell_1,\infty,p|x_0)=\frac{1}{D\alpha^2}\left(1-\frac{\cosh(\alpha(b-x_0))}{\cosh(\alpha b)}\mathrm{e}^{-\alpha\,\tanh(\alpha b)\ell_1}\right), \tag{67}$$

$$\tilde{F}(\infty,\ell_2,p|x_0)=\frac{1}{D\alpha^2}\left(1-\frac{\cosh(\alpha x_0)}{\cosh(\alpha b)}\mathrm{e}^{-\alpha\,\tanh(\alpha b)\ell_2}\right) \tag{68}$$

(see appendix B for some other properties of the functions Q_1 and Q_2).

3.6. Results in time domain

The above expressions determine the full propagator and marginal densities in Laplace domain with respect to time t. As it is quite common for diffusion-based quantities, representations in Laplace domain are more explicit and compact. A standard way to perform the Laplace inversion and thus to pass back to time domain consists in searching for the poles of the full propagator in the complex plane $p\in\mathbb{C}$. For instance, this computation is straightforward for the first term in equation (50) and yields the standard spectral expansion of the propagator $G_{\infty,\infty}(x,t|x_0)$ on the interval with absorbing endpoints. However, the analysis is more subtle for other terms. For example, the second term in front of $\delta(\ell_1)$ includes the function

$$\tilde{f}(p)=\mathrm{e}^{-C\ell_2}=\exp\left(-\ell_2\sqrt{p/D}\,\mathrm{ctanh}\left(\sqrt{p/D}b\right)\right).$$

While the poles of the factor in front of this exponential function in equation (50) are $p_n=-\pi^2n^2D/b^2$, the function $\tilde{f}(p)$ rapidly vanishes as $p\to p_n$ that prevents applying the residue theorem. In appendix C, we derive a semi-analytical formula for inverting such Laplace transforms. This formula is particularly valuable in the short-time limit. However, its practical implementation becomes numerically difficult at long times. For this reason, we applied the Talbot algorithm for numerical Laplace transform inversion. Further analysis of the long-time asymptotic behavior remains an interesting open problem.

Figure 2 shows the joint probability density $P(\circ,\ell_1,\ell_2,t|x_0)$ of two boundary local times ℓ_1 and ℓ_2 at the endpoints of the unit interval $(0,1)$. Here we present only the continuous part (i.e. the Laplace transform inversion of the three last terms in equation (53) that do not contain either $\delta(\ell_1)$, nor $\delta(\ell_2)$; in fact, the three other terms containing either of these δ's are simpler and can be presented separately). When the starting point x_0 is at the middle of the interval (top row), both endpoints are equally accessible, and $P(\circ,\ell_1,\ell_2,t|x_0)$ is symmetric with respect to exchange of ℓ_1 and ℓ_2. As time t increases, the maximum of the joint probability density moves along the diagonal $\ell_1=\ell_2$. In fact, in the long-time limit ($\sqrt{Dt}\gg b$), the diffusing particle has enough time to frequently encounter both endpoints, and the mean boundary local times grow linearly with t, see equation (33). As the variance also grows linearly with time according to equation (34), the maximum of the

J. Stat. Mech. (2020) 103205

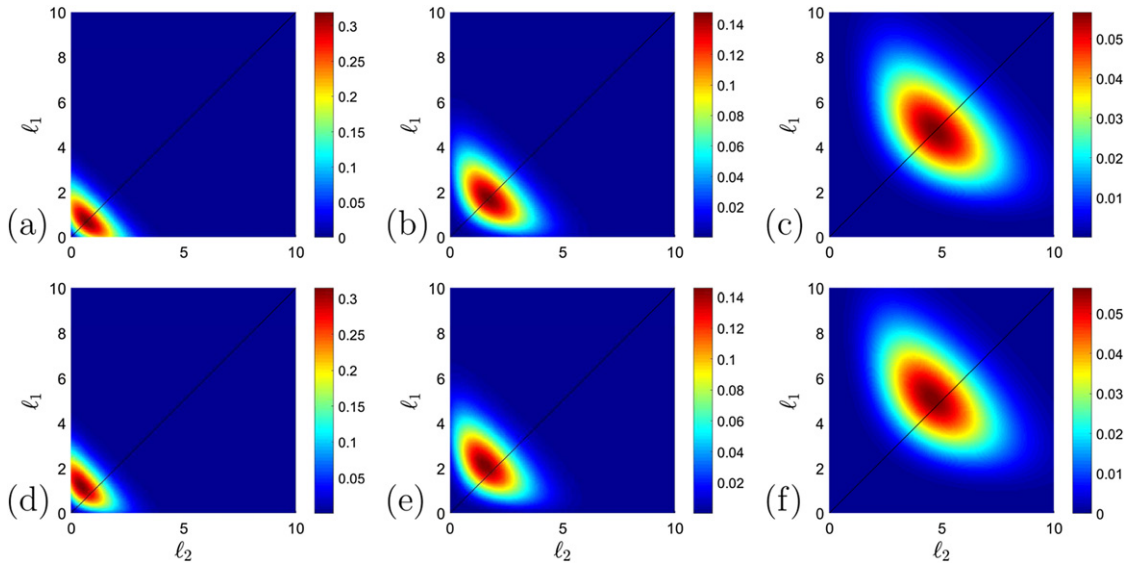

Figure 2. The continuous part of the joint probability density $P(\circ, \ell_1, \ell_2, t|x_0)$ of two boundary local times ℓ_1 and ℓ_2 at the endpoints of the unit interval $(0, 1)$, with $x_0 = 0.5$ (top row) and $x_0 = 0$ (bottom row), and three times: $t = 1$ (left column), $t = 2$ (middle column), and $t = 5$ (right column), with $D = 1$.

joint probability density spreads. If the particle starts on (or near) the left endpoint (bottom row), the joint probability density is shifted to larger values of ℓ_1. However, as time increases, the maximum progressively returns to the diagonal, as expected.

3.7. Extension to circular annulus and spherical shell

The computation for a circular annulus, $\Omega = \{\boldsymbol{x} \in \mathbb{R}^2 \,:\, a < |\boldsymbol{x}| < b\}$, and for a spherical shell, $\Omega = \{\boldsymbol{x} \in \mathbb{R}^3 \,:\, a < |\boldsymbol{x}| < b\}$, are very similar but technically more involved. In fact, the rotational symmetry of these domains allows one to separate variables and to expand the solution over Fourier harmonics (in 2D) or over spherical harmonics (in 3D). In turn, the radial propagator associated to each harmonic has an exact explicit form, which is similar to equation (23), see [63] and appendix D for details. As the dependence on q_1 and q_2 is exactly the same, one can apply the above technique to inverse the double Laplace transform. One gets then the radial part of the full propagator, $\tilde{P}_n(r, \ell_1, \ell_2, p|r_0)$ (corresponding to the nth harmonic). The structure of this radial part is similar to that of equation (50), even though the radius-dependent prefactors are different. For the sake of brevity, we do not provide explicit formulas here (see also [64]).

4. Variety of first-passage times

The derived joint probability densities allow one to investigate various FPTs. The distribution of a FPT τ is in general determined by the survival probability, $\mathbb{P}_{x_0}\{\tau > t\}$,

J. Stat. Mech. (2020) 103205

from which the probability density follows as $H(t|x_0) = -\partial_t \mathbb{P}_{x_0}\{\tau > t\}$. We will consider the latter quantity in the Laplace domain.

4.1. Conventional first-passage times

The distribution of the FPT to a perfectly or partially reactive target has been intensively studied in various settings [2, 37, 38, 44, 54, 66–79]. The most common FPT is the moment of the first arrival of the process to the boundary (or the target): $\tau = \inf\{t > 0 : \boldsymbol{X}_t \in \partial\Omega\}$. As the boundary local time remains zero until the first encounter, this FPT can also be formulated as $\tau = \inf\{t > 0 : \ell_t > 0\}$, i.e. the moment of the first crossing of the threshold 0 by the total boundary local time ℓ_t. In the case of the interval, the FPT to either of the boundaries Γ_1 and Γ_2 reads then

$$\tau = \tau_{\infty,\infty} = \inf\{t > 0 \,:\, \ell_t^1 + \ell_t^2 > 0\} = \inf\{t > 0 \,:\, \ell_t^1 > 0 \text{ or } \ell_t^2 > 0\}. \tag{69}$$

This FPT is determined by the Laplace-transformed survival probability $\tilde{S}_{\infty,\infty}(p|x_0)$ standing in front of $\delta(\ell_1)\delta(\ell_2)$ in equation (53):

$$\mathbb{P}_{x_0}\{\tau_{\infty,\infty} > t\} = \mathbb{P}_{x_0}\{\ell_t^1 = 0 \text{ and } \ell_t^2 = 0\} = S_{\infty,\infty}(t|x_0). \tag{70}$$

Similarly, one can consider the FPT to one endpoint, say, to Γ_2: $\tau_{0,\infty} = \inf\{t > 0 \,:\, \ell_t^2 > 0\}$. The condition $\ell_t^2 = 0$ is expressed by $\delta(\ell_2)$, which is present in the first and the third terms in equation (53). Integrating these terms over the marginal variable ℓ_1 from 0 to ∞, one gets

$$\begin{aligned}
\int_0^\infty \mathrm{d}t\, e^{-pt}\, \mathbb{P}_{x_0}\{\tau_{0,\infty} > t\} &= \int_0^\infty \mathrm{d}t\, e^{-pt}\, \mathbb{P}_{x_0}\{\ell_t^2 = 0\} \\
&= \int_0^\infty \mathrm{d}\ell_1 \left(\tilde{S}_{\infty,\infty}(p|x_0)\, \delta(\ell_1) + \frac{\cosh(\alpha b) - 1}{\alpha\, \sinh(\alpha b)} \frac{\sinh(\alpha(b - x_0))}{\sinh(\alpha b)} \frac{\mathrm{e}^{-C\ell_1}}{D} \right) \\
&= \tilde{S}_{\infty,\infty}(p|x_0) + \frac{(\cosh(\alpha b) - 1)}{D\alpha^2\, \cosh(\alpha b)} \frac{\sinh(\alpha(b - x_0))}{\sinh(\alpha b)} \\
&= \frac{1}{D\alpha^2} \left(1 - \frac{\cosh(\alpha x_0)}{\cosh(\alpha b)} \right) = \tilde{S}_{0,\infty}(p|x_0),
\end{aligned} \tag{71}$$

i.e. $\mathbb{P}_{x_0}\{\tau_{0,\infty} > t\} = S_{0,\infty}(t|x_0)$. Indeed, as we are not interested in the boundary local time ℓ_t^1 here, this is equivalent to setting Neumann boundary condition on Γ_1, as discussed above.

4.2. First reaction times

When both endpoints are partially absorbing with equal reactivities (i.e. $q_1 = q_2 = q$), the reaction time can be defined as $\tau_{q,q} = \inf\{t > 0 \,:\, \ell_t^1 + \ell_t^2 > \hat{\ell}\}$, i.e. the first moment when the total boundary local time exceeds a random independently distributed threshold $\hat{\ell}$ with the exponential distribution with the mean q: $\mathbb{P}\{\hat{\ell} > \ell\} = \mathrm{e}^{-q\ell}$ [33, 35, 46, 56]. Qualitatively, the exponentially distributed threshold $\hat{\ell}$ for surface reactions plays the

J. Stat. Mech. (2020) 103205

same role as an exponentially distributed lifetime of a particle for bulk reactions (see [46] for details). The distribution of this random reaction time is

$$\mathbb{P}_{x_0}\{\tau_{q,q} > t\} = S_{q,q}(t|x_0), \tag{72}$$

which is determined by the explicitly known $\tilde{S}_{q,q}(p|x_0)$ from equation (27). This is a common setting for partial reactivity.

The above setting can be naturally generalized to deal with distinct surface reactivity parameters q_1 and q_2. In this case, one has to consider two boundary local times separately, as encounters with Γ_1 and Γ_2 result in the reaction event in different ways. Here, we define

$$\tau_{q_1,q_2} = \inf\{t > 0 \,:\, \ell_t^1 > \hat{\ell}_1 \text{ or } \ell_t^2 > \hat{\ell}_2\}, \tag{73}$$

as the first moment when *either* of the boundary local times ℓ_t^1 and ℓ_t^2 exceeds its random threshold, $\hat{\ell}_1$ and $\hat{\ell}_2$, which are determined as independent exponential random variables with means q_1 and q_2, respectively. As boundary local times are nondecreasing processes, the event $\{\tau_{q_1,q_2} > t\}$ means that none of boundary local times exceeded its threshold:

$$\begin{aligned}\mathbb{P}_{x_0}\{\tau_{q_1,q_2} > t\} &= \mathbb{P}_{x_0}\left\{\ell_t^1 < \hat{\ell}_1 \text{ and } \ell_t^2 < \hat{\ell}_2\right\} \\ &= \int_0^\infty \mathrm{d}\ell_1 \int_0^\infty \mathrm{d}\ell_2\, P(\circ, \ell_1, \ell_2, t|x_0)\, \mathbb{P}\{\ell_1 < \hat{\ell}_1 \text{ and } \ell_2 < \hat{\ell}_2\} \\ &= \int_0^\infty \mathrm{d}\ell_1 \int_0^\infty \mathrm{d}\ell_2\, P(\circ, \ell_1, \ell_2, t|x_0)\, \mathrm{e}^{-q_1\ell_1}\, \mathrm{e}^{-q_2\ell_2} = S_{q_1,q_2}(t|x_0),\end{aligned} \tag{74}$$

where we applied equation (13) and used that $\hat{\ell}_1$ and $\hat{\ell}_2$ are independent exponential variables. In other words, this FPT time is determined by the survival probability $S_{q_1,q_2}(t|x_0)$ with Robin boundary conditions (16), as expected. While this extension is natural, we are not aware of earlier probabilistic definitions of the FPT τ_{q_1,q_2} with the help of two boundary local times, as in equation (73).

4.3. First-crossing times of two thresholds

The explicit form of the joint probability density $\tilde{P}(\circ, \ell_1, \ell_2, p|x_0)$ allows one to go far beyond the aforementioned FPTs. In particular, we will generalize the probability density of the first-crossing time for the total boundary local time ℓ_t derived in [46] (see appendix E for its properties).

First crossing by either of two boundary local times. The first natural extension consists in replacing exponential thresholds $\hat{\ell}_1$ and $\hat{\ell}_2$ in equation (73) by fixed thresholds ℓ_1 and ℓ_2. In other words, we are interested in the first moment when either of two boundary local times exceeds its threshold:

$$\tau_\cup = \inf\{t > 0 \,:\, \ell_t^1 > \ell_1 \text{ or } \ell_t^2 > \ell_2\}. \tag{75}$$

For instance, this FPT can describe the moment of the reaction, which is initiated when the particle either has visited at least ℓ_1/a times the vicinity of width a of the left target, or has visited at least ℓ_2/a times the a-vicinity of the right target. Qualitatively, this

J. Stat. Mech. (2020) 103205

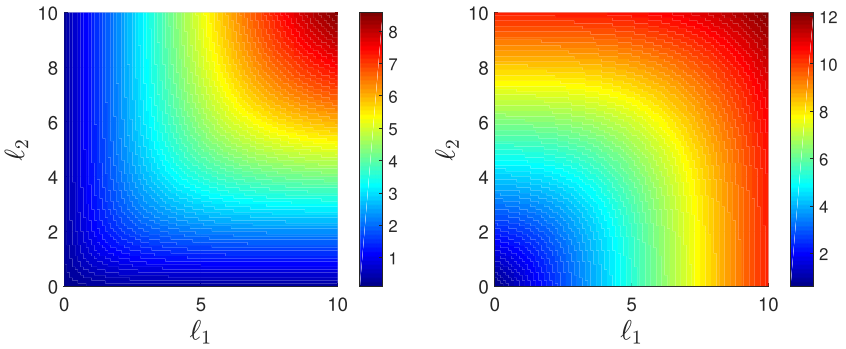

Figure 3. The mean first-crossing times $\mathbb{E}_{x_0}\{\tau_\cup\}$ (left) and $\mathbb{E}_{x_0}\{\tau_\cap\}$ (right) as functions of thresholds ℓ_1 and ℓ_2, with $b = 1$, $D = 1$, and $x_0 = 0.5$.

FPT describes a sort of minimal condition to produce the reaction event by either of the targets. If $\ell_1 = \ell_2 = \ell$, then $\tau_\cup$ is the first moment when $\max\{\ell_t^1, \ell_t^2\}$ exceeds ℓ.

The first-crossing time $\tau_\cup$ is determined by

$$S_\cup(t|x_0) = \mathbb{P}_{x_0}\{\tau_\cup > t\} = \mathbb{P}_{x_0}\left\{\ell_t^1 < \ell_1 \text{ and } \ell_t^2 < \ell_2\right\} = F(\ell_1, \ell_2, t|x_0), \tag{76}$$

where $F(\ell_1, \ell_2, t|x_0)$ is the joint cumulative probability function defined in equation (62). As the probability density of the first-crossing time, $H_\cup(t|x_0)$, is obtained by taking the time derivative of the survival probability (with negative sign), we get in the Laplace domain:

$$\tilde{H}_\cup(p|x_0) = 1 - p\tilde{F}(\ell_1, \ell_2, p|x_0), \tag{77}$$

with $\tilde{F}(\ell_1, \ell_2, p|x_0)$ given by equation (63). As usual, this function determines all positive integer moments of $\tau_\cup$:

$$\mathbb{E}_{x_0}\{\tau_\cup^m\} = (-1)^m \lim_{p\to 0} \frac{\partial^m}{\partial p^m} \tilde{H}_\cup(p|x_0). \tag{78}$$

In particular, the mean first-crossing time is

$$\begin{aligned}\mathbb{E}_{x_0}\{\tau_\cup\} = \tilde{F}(\ell_1, \ell_2, 0|x_0) &= \frac{x_0(b - x_0)}{2D} + \frac{b^2}{D}\hat{Q}_2(\ell_1/b, \ell_2/b) \\ &+ \frac{bx_0}{2D} Q_1(\ell_2/b\,; \sqrt{\ell_1/b}) + \frac{b(b - x_0)}{2D} Q_1(\ell_1/b\,; \sqrt{\ell_2/b}),\end{aligned} \tag{79}$$

where

$$\hat{Q}_2(z_1, z_2) = \lim_{a\to 1} \frac{Q_2(z_1, z_2\,; a)}{1 - a^2} = \int_0^{z_1} \mathrm{d}x_1 \int_0^{z_2} \mathrm{d}x_2\, \mathrm{e}^{-x_1 - x_2} I_0(2\sqrt{x_1 x_2}). \tag{80}$$

Figure 3 (left) illustrates the behavior of the mean first-crossing time $\mathbb{E}_{x_0}\{\tau_\cup\}$ as a function of ℓ_1 and ℓ_2.

As discussed in section 3.6, the analytical inversion of the Laplace transform like that in equation (77) is a challenging task. However, the short-time asymptotic behavior of

J. Stat. Mech. (2020) 103205

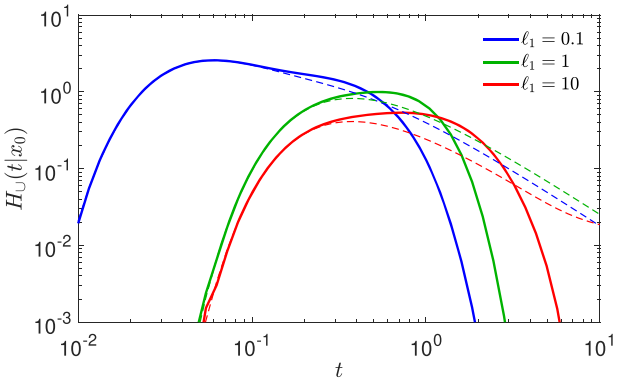

Figure 4. The probability density $H_\cup(t|x_0)$ of the first-crossing time $\tau_\cup$, with $b = 1$, $D = 1$, $x_0 = 0.5$, $\ell_2 = 1$, and three values of ℓ_1 as indicated in the plot. Solid lines show the numerical inversion of $\tilde{H}_\cup(p|x_0)$ via the Talbot algorithm, whereas dashed lines indicate the short-time asymptotic relation (82).

the probability density can be easily obtained. Using the asymptotic relations from appendix B, we get in the limit $p \to \infty$ for any $0 < x_0 < b$:

$$\tilde{F}(\ell_1, \ell_2, p|x_0) \simeq \frac{1}{p}\left(1 - \mathrm{e}^{-\alpha(x_0+\ell_1)} - \mathrm{e}^{-\alpha(b-x_0+\ell_2)}\right). \tag{81}$$

The short-time behavior of the probability density $H_\cup(t|x_0)$ follows then

$$H_\cup(t|x_0) \simeq \frac{1}{\sqrt{4\pi D t^3}}\left((x_0+\ell_1)\mathrm{e}^{-(x_0+\ell_1)^2/(4Dt)} + (b-x_0+\ell_2)\mathrm{e}^{-(b-x_0+\ell_2)^2/(4Dt)}\right). \tag{82}$$

Qualitatively, the first term represents the contribution of trajectories that rapidly reached the left endpoint (by crossing the distance x_0) and remained in its vicinity to increase the boundary local time ℓ_t^1 up to ℓ_1. Similarly, the second term accounts for the trajectories that reached the right endpoint and stayed nearby.

Figure 4 presents three probability densities $H_\cup(t|x_0)$ for $\ell_2 = 1$ and three values of ℓ_1: 0.1, 1, and 10. One first notes that the short-time relation (82) is in excellent agreement with the numerical inversion of $\tilde{H}_\cup(p|x_0)$ via the Talbot algorithm. As $\tau_\cup$ characterizes the first moment when either of two boundary local times crosses its threshold, the density $H_\cup(t|x_0)$ is shifted toward shorter times for $\ell_1 = 0.1$. In fact, it is on average much faster for the boundary local time ℓ_t^1 to cross the threshold $\ell_1 = 0.1$ than for ℓ_t^2 to cross $\ell_2 = 1$. The opposite situation occurs for $\ell_1 = 10$, which takes longer to cross than $\ell_2 = 1$. This explains that the probability density $H_\cup(t|x_0)$ does not considerably change when ℓ_1 is increased from 1 to 10.

While the short-time behavior is available, getting the long-time asymptotic behavior of $H_\cup(t|x_0)$ remains an open problem (see the related discussion in appendix E for a similar problem in the case of the total boundary local time).

First crossing by both boundary local times. Alternatively, one can look at the first moment when both ℓ_t^1 and ℓ_t^2 exceed their thresholds:

$$\tau_\cap = \inf\{t > 0 \,:\, \ell_t^1 > \ell_1 \text{ and } \ell_t^2 > \ell_2\}. \tag{83}$$

J. Stat. Mech. (2020) 103205

In particular, if $\ell_1 = \ell_2 = \ell$, $\tau_\cap$ is the first moment when $\min\{\ell_t^1, \ell_t^2\}$ exceeds ℓ.

The first-crossing time $\tau_\cap$ is determined by

$$\begin{aligned} S_\cap(t|x_0) &= \mathbb{P}_{x_0}\{\tau_\cap > t\} = \mathbb{P}_{x_0}\left\{\ell_t^1 < \ell_1 \text{ or } \ell_t^2 < \ell_2\right\} \\ &= 1 - \mathbb{P}_{x_0}\left\{\ell_t^1 > \ell_1 \text{ and } \ell_t^2 > \ell_2\right\} = 1 - \int_{\ell_1}^{\infty} \mathrm{d}\ell_1' \int_{\ell_2}^{\infty} \mathrm{d}\ell_2'\, P(\circ, \ell_1', \ell_2', t|x_0) \\ &= F(\ell_1, \infty, t|x_0) + F(\infty, \ell_2, t|x_0) - F(\ell_1, \ell_2, t|x_0), \end{aligned} \tag{84}$$

where the first two terms correspond to marginal cumulative probability functions given by equation (67). In the Laplace domain, we get then

$$\begin{aligned} \tilde{H}_\cap(p|x_0) &= 1 - p\left(\tilde{F}(\ell_1, \infty, p|x_0) + \tilde{F}(\infty, \ell_2, p|x_0) - \tilde{F}(\ell_1, \ell_2, p|x_0)\right) \\ &= \frac{\cosh(\alpha(b - x_0))}{\cosh(\alpha b)} \mathrm{e}^{-\alpha \tanh(\alpha b)\ell_1} + \frac{\cosh(\alpha x_0)}{\cosh(\alpha b)} \mathrm{e}^{-\alpha \tanh(\alpha b)\ell_2} - \tilde{H}_\cup(p|x_0), \end{aligned} \tag{85}$$

where $\tilde{H}_\cup(p|x_0)$ is given by equation (77), and we used equation (67).

As previously, the density $\tilde{H}_\cap(p|x_0)$ determines all the positive integer moments of $\tau_\cap$, in particular,

$$\begin{aligned} \mathbb{E}_{x_0}\{\tau_\cap\} &= \tilde{F}(\ell_1, \infty, 0|x_0) + \tilde{F}(\infty, \ell_2, 0|x_0) - \tilde{F}(\ell_1, \ell_2, 0|x_0) \\ &= \frac{2b(\ell_1 + \ell_2) + 2b^2 - x_0^2 - (b - x_0)^2}{2D} - \mathbb{E}_{x_0}\{\tau_\cup\}, \end{aligned} \tag{86}$$

where $\mathbb{E}_{x_0}\{\tau_\cup\}$ is given by equation (79). Figure 3 (right) illustrates the behavior of the mean first-crossing time $\mathbb{E}_{x_0}\{\tau_\cap\}$ as a function of ℓ_1 and ℓ_2.

The short-time asymptotic behavior is determined from the limit $p \to \infty$. In this case, the leading terms that determined the behavior of $H_\cup(t|x_0)$, vanish, and one needs to keep terms up to the order of $\mathrm{e}^{-\alpha b}$. Skipping technical details, we get

$$\begin{aligned} H_\cap(t|x_0) \simeq \frac{1}{\sqrt{\pi D t^3}} \Big(&(x_0 + \ell_1 + \ell_2 + b)\mathrm{e}^{-(x_0+\ell_1+\ell_2+b)^2/(4Dt)} \\ &+ (2b - x_0 + \ell_1 + \ell_2)\mathrm{e}^{-(2b-x_0+\ell_1+\ell_2)^2/(4Dt)} \Big). \end{aligned} \tag{87}$$

Qualitatively, the first term represents the contribution of trajectories that rapidly reached the left endpoint (by crossing the distance x_0) and remained in its vicinity to increase the boundary local time ℓ_t^1 up to ℓ_1, then crossed the interval (by traveling distance b) to reach the right endpoint and remained nearby to increase ℓ_t^2 up to ℓ_2. Similarly, the second term accounts for the trajectories that first reached the right endpoint and then moved to the left endpoint.

Figure 5 illustrates the behavior of the probability density $H_\cap(t|x_0)$. As previously for $H_\cup(t|x_0)$, the short-time asymptotic relation (87) is accurate for small and moderate ℓ, while its range of applicability is limited for large ℓ. Expectedly, all curves are shifted to longer times as compared to figure 4 because the condition determining $\tau_\cap$ is more strict than that determining $\tau_\cup$.

J. Stat. Mech. (2020) 103205

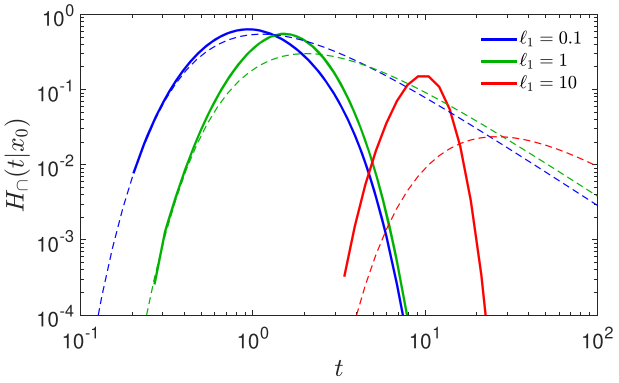

Figure 5. The probability density $H_\cap(t|x_0)$ of the first-crossing time $\tau_\cap$, with $b = 1$, $D = 1$, $x_0 = 0.5$, $\ell_2 = 1$, and three values of ℓ_1 as indicated in the plot. Solid lines show the numerical inversion of $\tilde{H}_\cap(p|x_0)$ via the Talbot algorithm, whereas dashed lines indicate the short-time asymptotic relation (87). Some points are missing at short times due to instabilities of the numerical inversion of the Laplace transform.

5. Discussion and conclusion

In this paper, we extended the approach relying on the concept of the boundary local time as a proxy for the number of encounters with the boundary that was recently developed to describe diffusion-mediated surface phenomena [46]. Our extension allows one to partition the boundary into regions with distinct reactivities and to characterize encounters with each region. For this purpose, we introduced the full propagator $P(\boldsymbol{x}, \ell_1, \ldots, \ell_m, t|\boldsymbol{x}_0)$ as the joint probability density of the position of the particle and of its multiple boundary local times on each boundary region. This propagator was then related via equation (11) to the conventional propagator $G_{q_1,\ldots,q_m}(\boldsymbol{x}, t|\boldsymbol{x}_0)$ satisfying Robin boundary conditions with parameters $q_1, \ldots, q_m$ on boundary regions Γ_i. The explicit implementation of the surface reactivities via the factors $\mathrm{e}^{-q_1\ell_1} \ldots \mathrm{e}^{-q_m\ell_m}$ in the expression (11) opens a way to investigate various surface reaction mechanisms such as catalysts' fooling or membrane degradation [80, 81]. In fact, the parameters q_i enter into the conventional propagator $G_{q_1,\ldots,q_m}(\boldsymbol{x}, t|\boldsymbol{x}_0)$ via the Robin boundary condition (7) that corresponds to the Poissonian type of surface reaction: at each encounter with Γ_i, the probability of the reaction event is the same. The factor $\mathrm{e}^{-q_i\ell_i}$ is thus the probability of no surface reaction on Γ_i, i.e. the probability $\mathbb{P}\{\hat{\ell}_i > \ell_t^i\}$ that the boundary local time ℓ_t^i does not exceed its random threshold $\hat{\ell}_i$ obeying the exponential distribution with the mean $1/q_i$. However, one can go beyond this conventional choice and consider a variety of surface reaction mechanisms characterized by any desired distribution of the threshold $\hat{\ell}_i$: $\mathbb{P}\{\hat{\ell}_i > \ell_i\} = \Psi_i(\ell_i)$ (see [46] for details). The generalized propagator describing the likelihood of finding the particle in $\boldsymbol{x}$ survived against such surface reactions will then be

$$G_{\mathrm{gen}}(\boldsymbol{x}, t|\boldsymbol{x}_0) = \int_0^\infty \mathrm{d}\ell_1\, \Psi_1(\ell_1) \ldots \int_0^\infty \mathrm{d}\ell_m\, \Psi_m(\ell_m)\, P(\boldsymbol{x}, \ell_1, \ldots, \ell_m, t|\boldsymbol{x}_0). \quad (88)$$

J. Stat. Mech. (2020) 103205

In this way, we extend the approach developed in [46] in order to implement various surface reaction mechanisms individually for each region Γ_i of the boundary. Several models of random thresholds and their consequences on the distribution of the reaction time were discussed in [46]. An interesting perspective consists in studying these models in the current setting with multiple boundary local times (and thus multiple thresholds $\hat{\ell}_i$). The exact formula (50) for the full propagator on the interval and its extensions to a circular annulus and a spherical shell will be particularly helpful.

Another interesting extension consists in studying the limit $m \to \infty$ of finer and finer partitions of the boundary $\partial\Omega$. As a sequence of piecewise constant functions can approximate a given function $q_{\boldsymbol{s}}$ characterizing the reactivity of the boundary, one can access the general case of a space-dependent reactivity, in which the propagator $G_{q_{\boldsymbol{s}}}(\boldsymbol{x}, t|\boldsymbol{x}_0)$ satisfies the Robin boundary condition:

$$\left(\partial_n G_{q_{\boldsymbol{s}}}(\boldsymbol{x}, t|\boldsymbol{x}_0)\right)_{\boldsymbol{x}=\boldsymbol{s}} + q_{\boldsymbol{s}}\, G_{q_{\boldsymbol{s}}}(\boldsymbol{s}, t|\boldsymbol{x}_0) = 0 \quad (\boldsymbol{s} \in \partial\Omega). \tag{89}$$

Indeed, equation (11) can formally be written as a sort of Feynman's path integral (here, we do not provide any rigorous statements but just sketch the main ideas):

$$G_{q_{\boldsymbol{s}}}(\boldsymbol{x}, t|\boldsymbol{x}_0) = \int \mathcal{D}\ell_{\boldsymbol{s}}\, \exp\left(-\int_{\partial\Omega} \mathrm{d}\boldsymbol{s}\, q_{\boldsymbol{s}}\, \ell_{\boldsymbol{s}}\right) P(\boldsymbol{x}, \ell_{\boldsymbol{s}}, t|\boldsymbol{x}_0) \tag{90}$$

$$= \mathbb{E}_{\boldsymbol{x}_0}\left\{\exp\left(-\int_{\partial\Omega} \mathrm{d}\boldsymbol{s}\, q_{\boldsymbol{s}}\, \ell_t^{\boldsymbol{s}}\right) \delta(\boldsymbol{X}_t - \boldsymbol{x})\right\}, \tag{91}$$

where $\ell_t^{\boldsymbol{s}}$ is the boundary local time in an infinitesimal vicinity of the boundary point $\boldsymbol{s}$. As $\ell_t^{\boldsymbol{s}}$ increases only when the particle hits a vicinity of the point $\boldsymbol{s}$, the integral over $\boldsymbol{s}$ can be re-arranged as

$$\int_{\partial\Omega} \mathrm{d}\boldsymbol{s}\, q_{\boldsymbol{s}}\, \ell_t^{\boldsymbol{s}} = \int_0^t q_{\boldsymbol{X}_{t'}}\, \mathrm{d}\ell_{t'}, \tag{92}$$

where $\mathrm{d}\ell_{t'}$ denotes increments of the total boundary local time ℓ_t on the whole boundary $\partial\Omega$. Using this relation, one gets a probabilistic representation

$$G_{q_{\boldsymbol{s}}}(\boldsymbol{x}, t|\boldsymbol{x}_0) = \mathbb{E}_{\boldsymbol{x}_0}\left\{\exp\left(-\int_0^t q_{\boldsymbol{X}_{t'}}\, \mathrm{d}\ell_{t'}\right) \delta(\boldsymbol{X}_t - \boldsymbol{x})\right\}, \tag{93}$$

which is more conventional for the mathematical literature on stochastic processes [82, 83]. On the other hand, a spectral expansion of the propagator $G_{q_{\boldsymbol{s}}}(\boldsymbol{x}, t|\boldsymbol{x}_0)$ in terms of the eigenfunctions of the operator $\mathcal{M}_p + q_{\boldsymbol{s}}$ was derived in [55]. Further mathematical analysis of this intricate relation presents an interesting perspective for future research.

We also discussed a variety of the FPTs associated to this problem. After identifying the conventional cases of perfectly and partially reactive targets, we introduced a new class of FPTs characterizing the moment of the first crossing of prescribed thresholds by two boundary local times. We derived the exact formulas for the Laplace-transformed probability densities of such first-crossing times $\tau_\cup$ and $\tau_\cap$. We also analyzed their short-time asymptotic behavior and obtained the mean values of these random variables. In

J. Stat. Mech. (2020) 103205

turn, getting the long-time asymptotic behavior, which is usually much simpler for FPTs, remains an open problem (see also discussion in appendix E). Further progress in this direction may potentially be achieved with the help of the Donsker–Varadhan large deviation theory [84, 85]. The obtained probability densities of the FPTs could then be used for implementing new surface reaction mechanisms via stopping conditions. Note that we focused on FPTs related to the joint probability density $P(\circ, \ell_1, \ell_2, t|x_0)$ of two boundary local times. Another perspective consists in extending the obtained results by using the full propagator $P(x, \ell_1, \ell_2, t|x_0)$ and thus conditioning on the arrival point.

While most explicit results were presented for the interval, an extension to a circular annulus and a spherical shell is straightforward. All three domains are often used as models in various physical, chemical and biological applications. For instance, diffusion in an interval can model diffusion-influenced reactions in layered structures (such as a slab); diffusion in a circular annulus can be relevant for cylinder-shaped confinements (e.g. the interior space of a bacterium which contains nucleotides in the middle and is surrounded by an outer membrane); similarly, diffusion in a spherical shell can model diffusive processes inside the cytosol surrounded by the cellular and nuclear membranes. Apart from these basic models and related applications, the analytical results of the paper shed a light on the elaborate statistics of two boundary local times. In particular, the intrinsic correlations between these two processes illustrate the difficulties in getting more explicit results for general domains. In this perspective, the present work makes the first steps on the way toward the full description of boundary encounters and related surface reactions.

Acknowledgments

The author is grateful to G Oshanin for fruitful discussions of the inverse Laplace transforms. A partial financial support from the Alexander von Humboldt Foundation through a Bessel Research Award is acknowledged.

Appendix A. Dirichlet-to-Neumann operator for an interval

The Dirichlet-to-Neumann operator and its spectral properties were employed to describe diffusion-mediated surface phenomena in [46] (see also [55]). For a domain $\Omega \subset \mathbb{R}^d$ with a smooth boundary $\partial\Omega$, the Dirichlet-to-Neumann operator $\mathcal{M}_p$ associates to each (appropriate) function f on the boundary $\partial\Omega$ another function g on that boundary such that $\mathcal{M}_p f = g = (\partial_n w)|_{\partial\Omega}$, where $w(\boldsymbol{x})$ is the solution of the modified Helmholtz equation $(p - D\Delta)w(\boldsymbol{x}) = 0$ in Ω with Dirichlet boundary condition $w|_{\partial\Omega} = f$. In other words, the operator $\mathcal{M}_p$ maps Dirichlet boundary condition $w|_{\partial\Omega} = f$ to Neumann boundary condition $(\partial_n w)|_{\partial\Omega} = g = \mathcal{M}_p f$ for the same solution $w(\boldsymbol{x})$ (see [46, 55] for further discussion and references).

A general solution of the modified Helmholtz equation on an interval $(0, b)$ can be written as

$$w(x) = c_1 \frac{\sinh(\alpha(b - x))}{\sinh(\alpha b)} + c_2 \frac{\sinh(\alpha x)}{\sinh(\alpha b)}, \tag{A.1}$$

J. Stat. Mech. (2020) 103205

with unknown coefficients c_1 and c_2. As any 'function' on the boundary of the interval can be represented by a two-dimensional vector $(f_1, f_2)^\dagger$ (with coefficients f_1 and f_2), the Dirichlet-to-Neumann operator acts here as a 2×2 matrix

$$\mathcal{M}_p f = \begin{pmatrix} \alpha \operatorname{ctanh}(\alpha b) & -\alpha/\sinh(\alpha b) \\ -\alpha/\sinh(\alpha b) & \alpha \operatorname{ctanh}(\alpha b) \end{pmatrix} \begin{pmatrix} f_1 \\ f_2 \end{pmatrix}. \tag{A.2}$$

One can recognize the parameters C and $E/2$ from equations (41) and (43) as the diagonal and non-diagonal elements of this matrix. The eigenvalues and eigenvectors of this matrix are:

$$\mu_1 = C - E/2 = \alpha \tanh(\alpha b/2), \quad v_1 = \frac{1}{\sqrt{2}}(1,\ 1)^\dagger, \tag{A.3}$$

$$\mu_2 = C + E/2 = \alpha \operatorname{ctanh}(\alpha b/2), \quad v_2 = \frac{1}{\sqrt{2}}(1,\ -1)^\dagger. \tag{A.4}$$

Using equation (51), one finds

$$V_1^{(p)}(x_0) = \frac{\sinh(\alpha(b-x_0)) + \sinh(\alpha x_0)}{\sqrt{2}\,\sinh(\alpha b)}, \tag{A.5}$$

$$V_2^{(p)}(x_0) = \frac{\sinh(\alpha(b-x_0)) - \sinh(\alpha x_0)}{\sqrt{2}\,\sinh(\alpha b)}, \tag{A.6}$$

where $V_n^{(p)}(x_0)$ were defined in [46] as projections of $\tilde{j}_{\infty,\infty}(s, p|x_0)$ onto the eigenfunctions of the Dirichlet-to-Neumann operator.

Using these expressions, we can compute the full propagator $\tilde{P}_{\rm tot}(x, \ell, p|x_0)$ in the case of equal reactivities ($q_1 = q_2$), which characterizes the total boundary local time $\ell_t = \ell_t^1 + \ell_t^2$ [46]:

$$\begin{aligned} D\tilde{P}_{\rm tot}(x, \ell, p|x_0) &= D\tilde{G}_{\infty,\infty}(x, p|x_0)\delta(\ell) + \sum_n V_n^{(p)}(x_0) V_n^{(p)}(x) \mathrm{e}^{-\mu_n^{(p)}\ell} \\ &= D\tilde{G}_{\infty,\infty}(x, p|x_0)\delta(\ell) + \mathrm{e}^{-C\ell} \\ &\quad \times \left(\frac{\sinh(\alpha(b-x_0))\sinh(\alpha(b-x)) + \sinh(\alpha x_0)\sinh(\alpha x)}{\sinh^2(\alpha b)} \cosh(E\ell/2) \right. \\ &\quad \left. - \frac{\sinh(\alpha(b-x_0))\sinh(\alpha x) + \sinh(\alpha x_0)\sinh(\alpha(b-x))}{\sinh^2(\alpha b)} \sinh(E\ell/2) \right), \end{aligned} \tag{A.7}$$

where $\tilde{G}_{\infty,\infty}(x, p|x_0)$ is given by equation (23). The marginal probability density of ℓ_t in the Laplace domain reads

$$\begin{aligned} \tilde{P}_{\rm tot}(\circ, \ell, p|x_0) &= \tilde{S}_{\infty,\infty}(p|x_0)\delta(\ell) + \frac{\cosh(\alpha b) - 1}{\alpha\ \sinh(\alpha b)} \frac{\sinh(\alpha x_0) + \sinh(\alpha(b-x_0))}{\sinh(\alpha b)} \\ &\quad \times \frac{\mathrm{e}^{-(C-E/2)\ell}}{D}. \end{aligned} \tag{A.8}$$

J. Stat. Mech. (2020) 103205

The cumulative probability function of ℓ_t is

$$\tilde{F}_{\rm tot}(\ell,p|x_0)=\frac{1}{D\alpha^2}\left(\Theta(\ell)+\frac{\sinh(\alpha x_0)+\sinh(\alpha(b-x_0))}{\sinh(\alpha b)}\left(1-\Theta(\ell)-{\rm e}^{-(C-E/2)\ell}\right)\right), \tag{A.9}$$

where the derivative of the Heaviside function $\Theta(\ell)$ yields $\delta(\ell)$ in the above probability density.

In addition to the above Dirichlet-to-Neumann operator, one can consider other versions of this operator, which can give complementary insights on this problem. The first one consists in restricting the operator to one endpoint, e.g. on $\Gamma_2=\{b\}$. In other words, the modified operator acts on functions defined only on Γ_2 (here, as the boundary Γ_2 consists of one point, this 'functional' space is one-dimensional), while the solution is fixed to 0 at the other endpoint. This is equivalent to fixing $c_1\equiv 0$ in equation (A.1), and the action of the modified Dirichlet-to-Neumann operator reads

$$\mathcal{M}_p^D f=\left(\partial_n\frac{\sinh(\alpha x)}{\sinh(\alpha b)}f\right)\Big|_{x=b}=\alpha\,{\rm ctanh}(\alpha b)f, \tag{A.10}$$

where $\alpha\,{\rm ctanh}(\alpha b)$ can be interpreted as the eigenvalue of this operator (corresponding to the eigenfunction $v=1$). As the space of 'functions' is one-dimensional (i.e. the 'function' f is just a scalar), this is the only eigenvalue of the operator.

The second modification consists in imposing Neumann boundary condition on one endpoint, e.g. on $\Gamma_1=\{0\}$. A general solution of the modified Helmholtz equation with Neumann condition at $x=0$ and Dirichlet condition at $x=b$ reads

$$w(x)=c\,\frac{\cosh(\alpha x)}{\cosh(\alpha b)}, \tag{A.11}$$

and the action of the modified Dirichlet-to-Neumann operator on a 'function' f on Γ_2 is

$$\mathcal{M}_p^N f=\left(\partial_n\frac{\cosh(\alpha x)}{\cosh(\alpha b)}f\right)\Big|_{x=b}=\alpha\ \tanh(\alpha b)f. \tag{A.12}$$

Here, $\alpha\tanh(\alpha b)$ is the eigenvalue of this operator corresponding to the eigenfunction $v=1$.

Appendix B. Some properties of functions Q_1 and Q_2

The functions $Q_1(z\,;a)$ and $Q_2(z_1,z_2\,;a)$ can be computed numerically from their definition in equation (65). In this appendix, we provide some additional representations and asymptotic properties.

Using the representation:

$$I_0(z)=\frac{1}{\pi}\int_0^\pi {\rm d}\theta\,\exp(x\ \cos\ \theta), \tag{B.1}$$

J. Stat. Mech. (2020) 103205

one can write

$$Q_1(z\,;a) = \mathrm{e}^{-a^2}\int_0^z \mathrm{d}x\,\mathrm{e}^{-x}\,I_0(2a\sqrt{x}) = \mathrm{e}^{-a^2}\int_0^z \mathrm{d}x\,\mathrm{e}^{-x}\sum_{n=0}^{\infty}\frac{(2a)^{2n}}{(2n)!}c_n\,x^n, \tag{B.2}$$

where

$$c_n = \frac{1}{\pi}\int_0^{\pi}\mathrm{d}\theta\,[\cos(\theta)]^{2n} = \frac{(2n-1)!!}{2^n\,n!}. \tag{B.3}$$

We get then

$$Q_1(z\,;a) = \mathrm{e}^{-a^2}\sum_{n=0}^{\infty}\frac{(2a)^{2n}}{(2n)!}c_n\,\left(n!\,\mathrm{e}^{-z}\sum_{k=0}^{n}\frac{z^k}{k!}\right) = \mathrm{e}^{-z-a^2}\sum_{n=0}^{\infty}\frac{a^{2n}}{n!}\sum_{k=0}^{n}\frac{z^k}{k!}. \tag{B.4}$$

Note also that the finite sum over k in equation (B.4) can be written in terms of the upper incomplete gamma function so that

$$Q_1(z\,;a) = \mathrm{e}^{-a^2}\sum_{n=0}^{\infty}\frac{a^{2n}}{n!}\,\frac{\Gamma(n+1,z)}{n!}. \tag{B.5}$$

Similarly, the double integral reads

$$\begin{aligned} Q_2(z_1,z_2\,;a) &= (1-a^2)\int_0^{z_1}\mathrm{d}x_1\int_0^{z_2}\mathrm{d}x_2\,\mathrm{e}^{-x_1-x_2}I_0(2a\sqrt{x_1x_2}) \\ &= (1-a^2)\mathrm{e}^{-z_1-z_2}\sum_{n=0}^{\infty}a^{2n}\left(\sum_{k=0}^{n}\frac{z_1^k}{k!}\right)\left(\sum_{k=0}^{n}\frac{z_2^k}{k!}\right). \end{aligned} \tag{B.6}$$

For large z, it is convenient to write

$$Q_1(z\,;a) = 1-\mathrm{e}^{-a^2}\int_z^{\infty}\mathrm{d}z\,\mathrm{e}^{-x}\,I_0(2a\sqrt{x}). \tag{B.7}$$

If in addition $a \ll 1/z$, then one can expand $I_0(z)$ in a Taylor series to get

$$Q_1(z\,;a) \simeq 1-\mathrm{e}^{-a^2-z}\left(1+(1+z)a^2+\ldots\right) \simeq 1-\mathrm{e}^{-z}(1+za^2+O(a^4)). \tag{B.8}$$

In the limit $p\to\infty$, one gets then

$$Q_1\left(C\ell_2\,;\sqrt{C\ell_1}\,\mathrm{sech}(\alpha b)\right) \simeq 1-\mathrm{e}^{-\alpha\ell_2}+O(\mathrm{e}^{-2\alpha b}), \tag{B.9}$$

$$Q_1\left(C\ell_1\,;\sqrt{C\ell_2}\,\mathrm{sech}(\alpha b)\right) \simeq 1-\mathrm{e}^{-\alpha\ell_1}+O(\mathrm{e}^{-2\alpha b}). \tag{B.10}$$

Noting that

$$Q_2(z_1,\infty\,;a) = 1-\mathrm{e}^{-(1-a^2)z_1}, \qquad Q_2(\infty,z_2\,;a) = 1-\mathrm{e}^{-(1-a^2)z_2}, \tag{B.11}$$

J. Stat. Mech. (2020) 103205

one gets for very small a:

$$\begin{aligned} Q_2(z_1,z_2\,;a) &= 1-\mathrm{e}^{-(1-a^2)z_1}-\mathrm{e}^{-(1-a^2)z_2}+(1-a^2)\int_{z_1}^{\infty}\mathrm{d}x_1\int_{z_2}^{\infty}\mathrm{d}x_2\,\mathrm{e}^{-x_1-x_2}I_0(2a\sqrt{x_1x_2}) \\ &\approx 1-\mathrm{e}^{-(1-a^2)z_1}-\mathrm{e}^{-(1-a^2)z_2}+(1-a^2)\mathrm{e}^{-z_1-z_2}\left(1+a^2(1+z_1)(1+z_2)+O(a^4)\right) \\ &= (1-\mathrm{e}^{-z_1})(1-\mathrm{e}^{-z_2})-(z_1\mathrm{e}^{-z_1}+z_2\mathrm{e}^{-z_2}-(z_1z_2+z_1+z_2)\mathrm{e}^{-z_1-z_2})\,a^2+O(a^4). \end{aligned}$$

In the limit $p\to\infty$, one has

$$Q_2\left(C\ell_1,C\ell_2\,;\mathrm{sech}(\alpha b)\right)\simeq 1-\mathrm{e}^{-\alpha\ell_1}-\mathrm{e}^{-\alpha\ell_2}+\mathrm{e}^{-\alpha(\ell_1+\ell_2)}+O(\mathrm{e}^{-2\alpha b}). \tag{B.12}$$

Appendix C. Two Laplace transform inversion formulas

In this appendix, we aim at computing two classes of the inverse Laplace transform:

$$U(t)=\mathcal{L}^{-1}\left\{\exp(-xf(\mathrm{e}^{-a\sqrt{p}}))\right\}, \tag{C.1}$$

$$V(t)=\mathcal{L}^{-1}\left\{\exp(-xa\sqrt{p}f(\mathrm{e}^{-a\sqrt{p}}))\right\}, \tag{C.2}$$

where $a>0$, $x>0$, and $f(z)$ is an analytic function.

The first step consists in replacing $a\sqrt{p}$ by p with the help of the following identity

$$\mathcal{L}\left\{\int_0^{\infty}\mathrm{d}\tau\,F(t,\tau)\,h(\tau)\right\}(p)=\int_0^{\infty}\mathrm{d}\tau\,\mathrm{e}^{-a\tau\sqrt{p}}\,h(\tau)=\mathcal{L}\{h\}(a\sqrt{p})=\tilde{h}(a\sqrt{p}), \tag{C.3}$$

where $h(t)$ is a given function, and

$$F(t,\tau)=\frac{a\tau}{\sqrt{4\pi t^3}}\,\mathrm{e}^{-a^2\tau^2/(4t)}. \tag{C.4}$$

Inverting this identity, we get another identity for a given function $\tilde{h}(p)$:

$$\mathcal{L}^{-1}\{\tilde{h}(a\sqrt{p})\}=\int_0^{\infty}\mathrm{d}\tau\,F(t,\tau)\,\mathcal{L}^{-1}\{\tilde{h}\}(\tau). \tag{C.5}$$

Using this representation, we have

$$U(t)=\int_0^{\infty}\mathrm{d}\tau\,F(t,\tau)\,\mathcal{L}^{-1}\left\{\exp(-xf(\mathrm{e}^{-p}))\right\}(\tau). \tag{C.6}$$

In the second step, we expand the exponential function and use the Taylor series

$$[f(z)]^n=\sum_{k=0}^{\infty}f_{n,k}\,z^k \tag{C.7}$$

to write

J. Stat. Mech. (2020) 103205

$$U(t) = \int_0^\infty \mathrm{d}\tau\, F(t,\tau)\, \mathcal{L}^{-1}\left\{\sum_{n,k} \frac{(-x)^n}{n!}\, f_{n,k}\, \mathrm{e}^{-kp}\right\}(\tau)$$
$$= \sum_{k=0}^\infty F(t,k) \sum_{n=0}^\infty \frac{(-x)^n}{n!}\, \frac{1}{k!} \left(\frac{\partial^k}{\partial z^k}[f(z)]^n\right)_{z=0},$$

where we used that the inverse Laplace transform of e^{-kp} is $\delta(\tau - k)$. Finally, the series over n yields the exponential function, so that we conclude

$$\mathcal{L}^{-1}\left\{\exp(-xf(\mathrm{e}^{-a\sqrt{p}}))\right\}(t) = \frac{a}{\sqrt{4\pi t^3}} \sum_{k=1}^\infty \frac{\mathrm{e}^{-a^2k^2/(4t)}}{(k-1)!} \lim_{z\to 0}\left(\frac{\partial^k}{\partial z^k} \exp(-xf(z))\right). \quad \text{(C.8)}$$

This partly explicit expression allows one to easily compute the short-time behavior by keeping only the first term with $k = 1$.

In the same way, we can compute the inverse Laplace transform $V(t)$:

$$V(t) = \int_0^\infty \mathrm{d}\tau\, F(t,\tau) \mathcal{L}^{-1}\left\{\sum_{n,k} \frac{(-x)^n\, p^n}{n!}\, f_{n,k}\right\}(\tau)$$
$$= \sum_{n,k} \frac{(-x)^n}{n!}\, f_{n,k} \int_0^\infty \mathrm{d}\tau\, F(t,\tau)\, \delta^{(n)}(\tau - k) = \sum_{n,k} \frac{x^n}{n!}\, f_{n,k} \left(\frac{\partial^n}{\partial \tau^n} F(t,\tau)\right)_{\tau=k}$$
$$= \sum_{n,k} \frac{x^n}{n!}\, \frac{1}{k!} \left(\frac{\partial^k}{\partial z^k}[f(z)]^n\right)_{z=0} \left(\frac{\partial^n}{\partial \tau^n} F(t,\tau)\right)_{\tau=k},$$

where $\delta^{(n)}(z)$ is the nth derivative of the Dirac distribution. Next, we expand the function $F(t,\tau)$ into a Taylor series and evaluate its derivatives with respect to τ:

$$V(t) = \sum_{n=0}^\infty \sum_{k=0}^\infty \frac{x^n}{n!}\, \frac{1}{k!} \left(\frac{\partial^k}{\partial z^k}[f(z)]^n\right)_{z=0} B \sum_{j=0}^\infty \frac{(-A)^j}{j!}\, k^{2j+1-n}\, \frac{(2j+1)!}{(2j+1-n)!},$$

where $B = a/\sqrt{4\pi t^3}$ and $A = a^2/(4t)$ (note that some terms in this sum are strictly zero, e.g. when $2j + 1 \leqslant n$). Exchanging the order of summations over n and j, one realizes that the sum over n is the binomial expansion:

$$V(t) = B \lim_{z\to 0} \sum_{k=0}^\infty \frac{1}{k!} \frac{\partial^k}{\partial z^k} \sum_{j=0}^\infty \frac{(-A)^j}{j!} \sum_{n=0}^\infty [xf(z)]^n\, k^{2j+1-n} \frac{(2j+1)!}{n!\,(2j+1-n)!}$$
$$= B \lim_{z\to 0} \sum_{k=0}^\infty \frac{1}{k!} \frac{\partial^k}{\partial z^k} \sum_{j=0}^\infty \frac{(-A)^j}{j!} (k + xf(z))^{2j+1}$$
$$= B \lim_{z\to 0} \sum_{k=0}^\infty \frac{1}{k!} \frac{\partial^k}{\partial z^k} (k + xf(z)) \exp\left(-A(k + xf(z))^2\right).$$

J. Stat. Mech. (2020) 103205

We conclude that

$$\mathcal{L}^{-1}\left\{\exp(-xa\sqrt{p}f(\mathrm{e}^{-a\sqrt{p}}))\right\}(t) = \frac{a}{\sqrt{4\pi t^3}}\lim_{z\to 0}\sum_{k=0}^{\infty}\frac{1}{k!}\frac{\partial^k}{\partial z^k}\left((k+xf(z))\mathrm{e}^{-a^2(k+xf(z))^2/(4t)}\right). \tag{C.9}$$

Keeping only the term with $k=0$, one gets the short-time asymptotic behavior:

$$V(t) \simeq \frac{axf(0)}{\sqrt{4\pi t^3}}\,\mathrm{e}^{-a^2x^2[f(0)]^2/(4t)}. \tag{C.10}$$

In the trivial case $f(z)=1$, equation (C.9) immediately yields the classical expression

$$\mathcal{L}^{-1}\left\{\exp(-xa\sqrt{p})\right\}(t) = \frac{ax}{\sqrt{4\pi t^3}}\,\mathrm{e}^{-a^2x^2/(4t)}. \tag{C.11}$$

Appendix D. The conventional propagator in two and three dimensions

The Laplace-transformed conventional propagator has an explicit form in two and three dimensions due to the separation of variables. Following [63], the radial part of the propagator in both cases reads as

$$\tilde{G}_{q_1,q_2}(r,p|r_0) = \frac{-1}{\alpha V W(\alpha r_0)\,\omega(r_0)} \times \begin{cases} v^b(r_0)\,v^a(r) & (a\leqslant r\leqslant r_0\leqslant b),\\ v^b(r)\,v^a(r_0) & (a\leqslant r_0\leqslant r\leqslant b),\end{cases} \tag{D.1}$$

where $W(z)=\mathcal{K}(z)\mathcal{I}'(z)-\mathcal{I}(z)\mathcal{K}'(z)$, $\omega(r_0)$ is the weighting factor,

$$v^a(r) = (\alpha\mathcal{K}'(\alpha a)-q_1\mathcal{K}(\alpha a))\,\mathcal{I}(\alpha r)-(\alpha\mathcal{I}'(\alpha a)-q_1\mathcal{I}(\alpha a))\,\mathcal{K}(\alpha r), \tag{D.2}$$

$$v^b(r) = (\alpha\mathcal{K}'(\alpha b)+q_2\mathcal{K}(\alpha b))\,\mathcal{I}(\alpha r)-(\alpha\mathcal{I}'(\alpha b)+q_2\mathcal{I}(\alpha b))\,\mathcal{K}(\alpha r), \tag{D.3}$$

$$V = (\alpha\mathcal{K}'(\alpha a)-q_1\mathcal{K}(\alpha a))\,(\alpha\mathcal{I}'(\alpha b)+q_2\mathcal{I}(\alpha b)) - (\alpha\mathcal{I}'(\alpha a)-q_1\mathcal{I}(\alpha a))\,(\alpha\mathcal{K}'(\alpha b)+q_2\mathcal{K}(\alpha b)), \tag{D.4}$$

and $\mathcal{I}$ and $\mathcal{K}$ are appropriate functions.

In two dimensions, one has

$$\mathcal{I}(z)=I_n(z), \qquad \mathcal{K}(z)=K_n(z), \qquad W(z)=1/z, \qquad \omega(r_0)=r_0, \tag{D.5}$$

where $I_n(z)$ and $K_n(z)$ are modified Bessel functions of the first and second kind, respectively. The Laplace-transformed propagator is then

$$\tilde{G}_{q_1,q_2}(\boldsymbol{x},p|\boldsymbol{x}_0) = \frac{1}{2\pi D}\sum_{n=-\infty}^{\infty}\mathrm{e}^{\mathrm{i}n(\phi-\phi_0)}\,\tilde{G}^{(n)}_{q_1,q_2}(r,p|r_0), \tag{D.6}$$

where $\boldsymbol{x}=(r,\phi)$ and $\boldsymbol{x}_0=(r_0,\phi_0)$ in polar coordinates, and the superscript (n) refers to the nth Fourier harmonic.

J. Stat. Mech. (2020) 103205

In three dimensions, one has

$$\mathcal{I}(z) = i_n(z), \qquad \mathcal{K}(z) = k_n(z), \qquad W(z) = 1/z^2, \qquad \omega(r_0) = r_0^2, \tag{D.7}$$

where $i_n(z)$ and $k_n(z)$ are modified spherical Bessel functions of the first and second kind, respectively. The Laplace-transformed propagator then reads

$$\tilde{G}_{q_1,q_2}(\boldsymbol{x}, p|\boldsymbol{x}_0) = \frac{1}{4\pi D}\sum_{n=0}^{\infty}(2n+1)P_n\left(\frac{(\boldsymbol{x}\cdot\boldsymbol{x}_0)}{|\boldsymbol{x}|\,|\boldsymbol{x}_0|}\right)\tilde{G}^{(n)}_{q_1,q_2}(r, p|r_0), \tag{D.8}$$

where $P_n(z)$ are Legendre polynomials, $r = |\boldsymbol{x}|$, and $r_0 = |\boldsymbol{x}_0|$.

In both cases, the dependence of the propagator on q_1 and q_2 is identical to that in the one-dimensional case. As a consequence, the inversion of the double Laplace transform with respect to q_1 and q_2 of each radial propagator can be performed explicitly, and then the obtained contributions can be summed up according to equations (D.6) and (D.8).

Appendix E. First-crossing time for the total boundary local time

In this appendix, we study the distribution of the first-crossing time τ of a given threshold ℓ by the total boundary local time $\ell_t = \ell_t^1 + \ell_t^2$ on the interval $(0, b)$. As discussed in section 4, the Laplace-transformed probability density $\tilde{H}(p|x_0)$ of τ is determined by the Laplace-transformed cumulative probability function $\tilde{F}_{\rm tot}(\ell, p|x_0)$ given by equation (A.9):

$$\begin{aligned}\mathbb{E}_{x_0}\{\mathrm{e}^{-p\tau}\} &= \tilde{H}(p|x_0) = 1 - p\tilde{F}_{\rm tot}(\ell, p|x_0) \\ &= \left(\frac{\sinh(\alpha x_0) + \sinh(\alpha(b-x_0))}{\sinh(\alpha b)}\right)\mathrm{e}^{-\alpha\,\tanh(\alpha b/2)\ell},\end{aligned} \tag{E.1}$$

where we assumed $\ell > 0$ to get a simpler expression (given that $\ell = 0$ corresponds to the well-studied case of the FPT to either of endpoints). The series expansion of this expression for $p \to 0$ allows one to compute the moments of τ:

$$\mathbb{E}_{x_0}\{\tau^m\} = (-1)^m \lim_{p\to 0}\frac{\partial^m}{\partial p^m}\tilde{H}(p|x_0). \tag{E.2}$$

In particular, we find the mean and the variance as

$$\mathbb{E}_{x_0}\{\tau\} = \frac{x_0(b-x_0) + \ell b}{2D}, \qquad \sigma_\tau^2 = \frac{x_0(b-x_0)(2x_0^2 - 2bx_0 + b^2) + \ell b^3}{12D^2}. \tag{E.3}$$

In both expressions, the first term (without ℓ) represents the contribution from the FPT to either of endpoints, whereas the second term accounts for multiple reflections. Indeed, the first-crossing time τ can be split into two independent contributions: the FPT to the endpoints, and the first-crossing time starting from the endpoint. Setting $x_0 = 0$ to cancel the conventional contribution from the FPT, we see that both the mean and the variance grow linearly with ℓ. As a consequence, the relative standard deviation, $\sigma_\tau/\mathbb{E}_{x_0}\{\tau\} = \sqrt{b/(3\ell)}$, decreases as ℓ grows.

J. Stat. Mech. (2020) 103205

As briefly mentioned in section 3.6, the standard tools for the Laplace transform inversion (such as the residue theorem) fail here because the exponential function in equation (E.1) exhibits essential singularities. For the sake of clarify, we set $x_0 = 0$ and consider

$$\tilde{H}(p|0) = \mathrm{e}^{-\alpha \tanh(\alpha b/2)\ell}. \tag{E.4}$$

Once its inverse, $H(t|0)$, is known, $H(t|x_0)$ can be obtained as a convolution of $H(t|0)$ with the inverse of the prefactor in parentheses in equation (E.1), which is well known (and can be easily obtained via the residue theorem).

In appendix C, we derived a semi-analytical formula (C.9) for inverting functions such as $\tilde{H}(p|0)$. Setting $x = \ell/b$ and $a = b/\sqrt{D}$ into this formula, we get

$$H(t|0) = \frac{1}{\sqrt{4\pi D t^3}} \lim_{z\to 0} \sum_{k=0}^{\infty} \frac{1}{k!} \frac{\partial^k}{\partial z^k} \left((bk + \ell f(z))\, \mathrm{e}^{-(bk+\ell f(z))^2/(4Dt)} \right), \tag{E.5}$$

where $f(z) = (1-z)/(1+z)$. The short-time behavior of this density is obtained by keeping only the term with $k = 0$:

$$H(t|0) \simeq \frac{\ell\, \mathrm{e}^{-\ell^2/(4Dt)}}{\sqrt{4\pi D t^3}} \quad (t \to 0). \tag{E.6}$$

In contrast, getting the long-time behavior is much more difficult. Without solving this open problem, we provide a rough approximation, which highlights the difficulties of the long-time limit.

Approximate computation in the long-time limit

As discussed in [33, 53], the boundary local time in a bounded domain is close to the Gaussian distribution in the long-time limit:

$$P_{\mathrm{tot}}(\circ, \ell, t|x_0) \simeq \frac{\exp(-\frac{(\ell - ct)^2}{2\beta t})}{\sqrt{2\pi\beta t}}, \tag{E.7}$$

where $c = D|\partial\Omega|/|\Omega| = 2D/b$ for an interval, and

$$\beta = -\left(\frac{D|\partial\Omega|}{|\Omega|}\right)^3 \lim_{p\to 0} \frac{\mathrm{d}^2\mu_1}{\mathrm{d}p^2} = \frac{2D}{3}, \tag{E.8}$$

where we used $\mu_1 = \alpha \tanh(\alpha b/2)$ for an interval, see equation (A.3). Note that this approximation does not depend on the starting point x_0, which is irrelevant in the long-time regime and will be omitted below. As a consequence, we get

$$\mathbb{P}\{\tau > t\} = \mathbb{P}\{\ell_t < \ell\} \simeq \frac{1}{2} \mathrm{erfc}\left(\frac{ct - \ell}{\sqrt{2\beta t}}\right), \tag{E.9}$$

from which

$$H(t) \simeq \frac{2D/b + \ell/t}{\sqrt{16\pi D t/3}} \exp\left(-\frac{(t - b\ell/(2D))^2}{b^2\, t/(3D)}\right) \quad (t \to \infty). \tag{E.10}$$

J. Stat. Mech. (2020) 103205

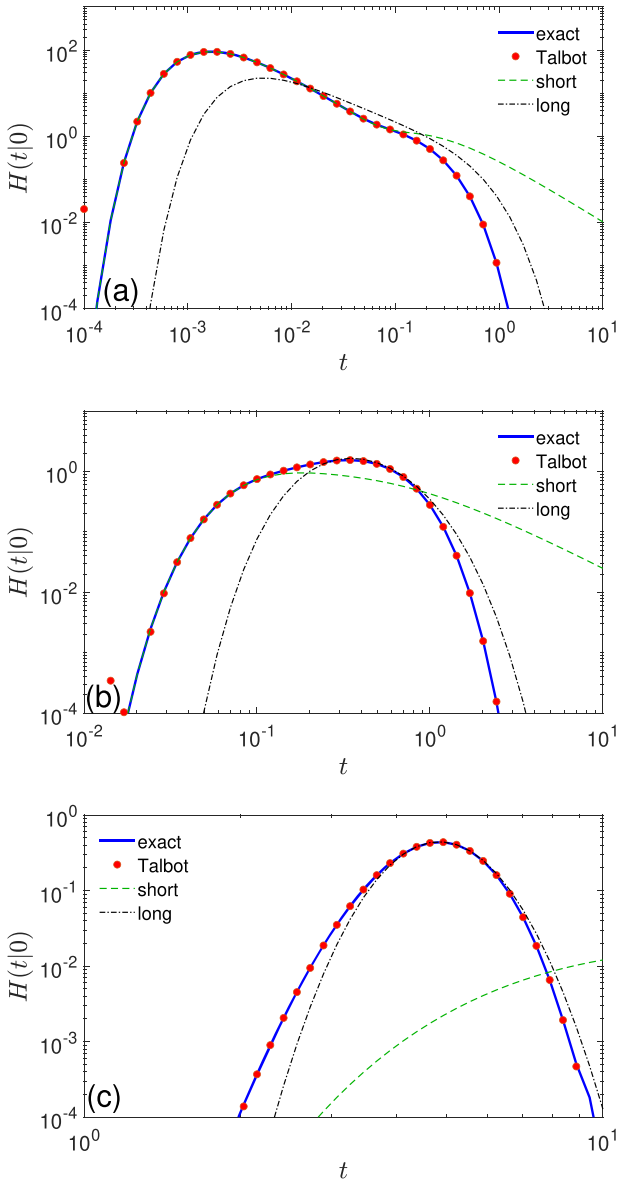

Figure 6. The probability density $H(t|0)$ of the first-crossing time τ of a threshold ℓ by the total boundary local time ℓ_t on the interval $(0, b)$, with $b = 1$, $D = 1$, and $\ell = 0.1$ (a), $\ell = 1$ (b), and $\ell = 10$ (c). Solid line presents the exact solution (E.5) truncated after $k = 20$, filled circles show the numerical inversion of equation (E.4) by the Talbot algorithm, dashed line indicates the short-time asymptotic relation (E.6), and dash-dotted line plots the long-time approximation (E.10).

Figure 6 shows the probability density $H(t|0)$ and its short-time and long-time approximations. First of all, one can note that the numerical inversion by the Talbot algorithm yields very accurate results, with only minor deviations at short times. As the threshold ℓ increases, the distribution of the first-crossing time is progressively shifted to longer times and becomes relatively narrower because the relative standard deviation

J. Stat. Mech. (2020) 103205

decreases. For $\ell = 0.1$ and $\ell = 1$, the short-time asymptotic formula (E.6) is accurate. In turn, for $\ell = 10$, even though this formula is accurate at short times, the probability density is so small due to the factor $\mathrm{e}^{-\ell^2/(4Dt)}$ that its range of validity is of limited interest. In contrast, the long-time approximation (E.10) fails for small and moderate ℓ but is getting more accurate for $\ell = 10$.

References

[1] Gardiner C W 1985 *Handbook of Stochastic Methods for Physics, Chemistry and the Natural Sciences* (Berlin: Springer)
[2] Redner S 2001 *A Guide to First Passage Processes* (Cambridge: Cambridge University Press)
[3] Schuss Z 2013 *Brownian Dynamics at Boundaries and Interfaces in Physics, Chemistry and Biology* (New York: Springer)
[4] Collins F C and Kimball G E 1949 Diffusion-controlled reaction rates *J. Colloid Sci.* **4** 425–37
[5] Sano H and Tachiya M 1979 Partially diffusion-controlled recombination *J. Chem. Phys.* **71** 1276–82
[6] Sano H and Tachiya M 1981 Theory of diffusion-controlled reactions on spherical surfaces and its application to reactions on micellar surfaces *J. Chem. Phys.* **75** 2870–8
[7] Hänggi P, Talkner P and Borkovec M 1990 Reaction-rate theory: fifty years after Kramers *Rev. Mod. Phys.* **62** 251–341
[8] Zhou H X and Zwanzig R 1991 A rate process with an entropy barrier *J. Chem. Phys.* **94** 6147–52
[9] Reguera D, Schmid G, Burada P S, Rubí J M, Reimann P and Hänggi P 2006 Entropic transport: kinetics, scaling, and control mechanisms *Phys. Rev. Lett.* **96** 130603
[10] Grebenkov D S and Oshanin G 2017 Diffusive escape through a narrow opening: new insights into a classic problem *Phys. Chem. Chem. Phys.* **19** 2723–39
[11] Berg H C and Purcell E M 1977 Physics of chemoreception *Biophys. J.* **20** 193–219
[12] Zwanzig R 1990 Diffusion-controlled ligand binding to spheres partially covered by receptors: an effective medium treatment *Proc. Natl Acad. Sci.* **87** 5856
[13] Zwanzig R and Szabo A 1991 Time dependent rate of diffusion-influenced ligand binding to receptors on cell surfaces *Biophys. J.* **60** 671–8
[14] Berezhkovskii A M, Makhnovskii Y A, Monine M I, Zitserman V Y and Shvartsman S Y 2004 Boundary homogenization for trapping by patchy surfaces *J. Chem. Phys.* **121** 11390
[15] Berezhkovskii A M, Monine M I, Muratov C B and Shvartsman S Y 2006 Homogenization of boundary conditions for surfaces with regular arrays of traps *J. Chem. Phys.* **124** 036103
[16] Muratov C B and Shvartsman S Y 2008 Boundary homogenization for periodic arrays of absorbers *Multiscale Model. Simul.* **7** 44–61
[17] Skvortsov A and Walker A 2014 Trapping of diffusive particles by rough absorbing surfaces: boundary smoothing approach *Phys. Rev.* E **90** 023202
[18] Skvortsov A T, Berezhkovskii A M and Dagdug L 2015 Boundary homogenization for a circle with periodic absorbing arcs. Exact expression for the effective trapping rate *J. Chem. Phys.* **143** 226101
[19] Dagdug L, Vázquez M-V, Berezhkovskii A M and Zitserman V Y 2016 Boundary homogenization for a sphere with an absorbing cap of arbitrary size *J. Chem. Phys.* **145** 214101
[20] Lindsay A E, Bernoff A J and Ward M J 2017 First passage statistics for the capture of a Brownian particle by a structured spherical target with multiple surface traps *Multiscale Model. Simul.* **15** 74–109
[21] Bernoff A J, Lindsay A E and Schmidt D D 2018 Boundary homogenization and capture time distributions of semipermeable membranes with periodic patterns of reactive sites *Multiscale Model. Simul.* **16** 1411–47
[22] Skvortsov A T, Berezhkovskii A M and Dagdug L 2019 Steady-state flux of diffusing particles to a rough boundary formed by absorbing spikes periodically protruding from a reflecting base *J. Chem. Phys.* **150** 194109
[23] Bénichou O, Moreau M and Oshanin G 2000 Kinetics of stochastically gated diffusion-limited reactions and geometry of random walk trajectories *Phys. Rev.* E **61** 3388–406
[24] Reingruber J and Holcman D 2009 Gated narrow escape time for molecular signalling *Phys. Rev. Lett.* **103** 148102
[25] Lawley S D and Keener J P 2015 A new derivation of Robin boundary conditions through homogenization of a stochastically switching boundary *SIAM J. Appl. Dyn. Syst.* **14** 1845–67
[26] Bressloff P C 2017 Stochastic switching in biology: from genotype to phenotype *J. Phys. A: Math. Theor.* **50** 133001

J. Stat. Mech. (2020) 103205

[27] Brownstein K R and Tarr C E 1979 Importance of classical diffusion in NMR studies of water in biological cells *Phys. Rev.* A **19** 2446–53
[28] Sapoval B 1994 General formulation of Laplacian transfer across irregular surfaces *Phys. Rev. Lett.* **73** 3314–6
[29] Filoche M and Sapoval B 1999 Can one hear the shape of an electrode? II. Theoretical study of the Laplacian transfer *Eur. Phys. J.* B **9** 755–63
[30] Sapoval B, Filoche M and Weibel E R 2002 Smaller is better—but not too small: a physical scale for the design of the mammalian pulmonary acinus *Proc. Natl Acad. Sci.* **99** 10411–6
[31] Grebenkov D S, Filoche M, Sapoval B and Felici M 2005 Diffusion-reaction in branched structures: theory and application to the lung acinus *Phys. Rev. Lett.* **94** 050602
[32] Grebenkov D S, Filoche M and Sapoval B 2006 Mathematical basis for a general theory of Laplacian transport towards irregular interfaces *Phys. Rev.* E **73** 021103
[33] Grebenkov D S 2007 Residence times and other functionals of reflected Brownian motion *Phys. Rev.* E **76** 041139
[34] Grebenkov D S 2010 Searching for partially reactive sites: analytical results for spherical targets *J. Chem. Phys.* **132** 034104
[35] Grebenkov D S 2019 Imperfect diffusion-controlled reactions *Chemical Kinetics: Beyond the Textbook* ed K Lindenberg, R Metzler and G Oshanin (Singapore: World Scientific)
[36] Rice S 1985 *Diffusion-Limited Reactions* (Amsterdam: Elsevier)
[37] Metzler R, Oshanin G and Redner S (ed) 2014 *First-Passage Phenomena and Their Applications* (Singapore: World Scientific)
[38] Lindenberg K, Metzler R and Oshanin G (ed) 2019 *Chemical Kinetics: Beyond the Textbook* (Singapore: World Scientific)
[39] Lauffenburger D A and Linderman J 1993 *Receptors: Models for Binding, Trafficking, and Signaling* (Oxford: Oxford University Press)
[40] Bouchaud J-P and Georges A 1990 Anomalous diffusion in disordered media: statistical mechanisms, models and physical applications *Phys. Rep.* **195** 127–293
[41] Grebenkov D S 2007 NMR survey of reflected Brownian motion *Rev. Mod. Phys.* **79** 1077–137
[42] Bénichou O, Loverdo C, Moreau M and Voituriez R 2011 Intermittent search strategies *Rev. Mod. Phys.* **83** 81–129
[43] Bressloff P C and Newby J M 2013 Stochastic models of intracellular transport *Rev. Mod. Phys.* **85** 135–96
[44] Bray A J, Majumdar S N and Schehr G 2013 Persistence and first-passage properties in nonequilibrium systems *Adv. Phys.* **62** 225–361
[45] Bénichou O and Voituriez R 2014 From first-passage times of random walks in confinement to geometry-controlled kinetics *Phys. Rep.* **539** 225–84
[46] Grebenkov D S 2020 Paradigm shift in diffusion-mediated surface phenomena *Phys. Rev. Lett.* **125** 078102
[47] Lévy P 1965 *Processus Stochastiques et Mouvement Brownien* (Paris: Gauthier-Villars)
[48] Ito K and McKean H P 1965 *Diffusion Processes and Their Sample Paths* (Berlin: Springer)
[49] Freidlin M 1985 *Functional Integration and Partial Differential Equations* (*Annals of Mathematics Studies*) (Princeton, NJ: Princeton University Press)
[50] Borodin A N and Salminen P 1996 *Handbook of Brownian Motion: Facts and Formulae* (Basel: Birkhäuser)
[51] Takacs L 1995 On the local time of the Brownian motion *Ann. Appl. Probab.* **5** 741
[52] Randon-Furling J and Redner S 2018 Residence time near an absorbing set *J. Stat. Mech.* 103205
[53] Grebenkov D S 2019 Probability distribution of the boundary local time of reflected Brownian motion in Euclidean domains *Phys. Rev.* E **100** 062110
[54] Grebenkov D S 2020 Diffusion toward non-overlapping partially reactive spherical traps: fresh insights onto classic problems *J. Chem. Phys.* **152** 244108
[55] Grebenkov D S 2019 Spectral theory of imperfect diffusion-controlled reactions on heterogeneous catalytic surfaces *J. Chem. Phys.* **151** 104108
[56] Grebenkov D S 2006 Partially reflected Brownian motion: a stochastic approach to transport phenomena *Focus on Probability Theory* ed L R Velle (New York: Nova Science Publishers) pp 135–69
[57] Grebenkov D S 2006 Scaling properties of the spread harmonic measures *Fractals* **14** 231–43
[58] Epstein C L and Schotland J 2008 The bad truth about Laplace's transform *SIAM Rev.* **50** 504–20
[59] Yuste S B, Abad E and Lindenberg K 2013 Exploration and trapping of mortal random walkers *Phys. Rev. Lett.* **110** 220603
[60] Meerson B and Redner S 2015 Mortality, redundancy, and diversity in stochastic search *Phys. Rev. Lett.* **114** 198101
[61] Grebenkov D S and Rupprecht J-F 2017 The escape problem for mortal walkers *J. Chem. Phys.* **146** 084106

J. Stat. Mech. (2020) 103205

[62] Thambynayagam R K M 2011 *The Diffusion Handbook: Applied Solutions for Engineers* (New York: McGraw-Hill)
[63] Grebenkov D S 2020 A physicist's guide to explicit summation formulas involving zeros of Bessel functions and related spectral sums *Rev. Math. Phys.* accepted
[64] Grebenkov D S 2020 Surface hopping propagator: an alternative approach to diffusion-influenced reactions *Phys. Rev.* E **102** 032125
[65] Debnath L 2016 The double Laplace transforms and their properties with applications to functional, integral and partial differential equations *Int. J. Appl. Comput. Math.* **2** 223–41
[66] Bénichou O and Voituriez R 2008 Narrow-escape time problem: time needed for a particle to exit a confining domain through a small window *Phys. Rev. Lett.* **100** 168105
[67] Bénichou O, Chevalier C, Klafter J, Meyer B and Voituriez R 2010 Geometry-controlled kinetics *Nat. Chem.* **2** 472–7
[68] Rupprecht J-F, Bénichou O, Grebenkov D S and Voituriez R 2015 Exit time distribution in spherically symmetric two-dimensional domains *J. Stat. Phys.* **158** 192–230
[69] Godec A and Metzler R 2016 Universal proximity effect in target search kinetics in the few-encounter limit *Phys. Rev.* X **6** 041037
[70] Godec A and Metzler R 2016 First passage time distribution in heterogeneity controlled kinetics: going beyond the mean first passage time *Sci. Rep.* **6** 20349
[71] Grebenkov D S, Metzler R and Oshanin G 2018 Towards a full quantitative description of single-molecule reaction kinetics in biological cells *Phys. Chem. Chem. Phys.* **20** 16393–401
[72] Agranov T and Meerson B 2018 Narrow escape of interacting diffusing particles *Phys. Rev. Lett.* **120** 120601
[73] Lanoiselée Y, Moutal N and Grebenkov D S 2018 Diffusion-limited reactions in dynamic heterogeneous media *Nat. Commun.* **9** 4398
[74] Artime O, Khalil N, Toral R and San Miguel M 2018 First-passage distributions for the one-dimensional Fokker–Planck equation *Phys. Rev.* E **98** 042143
[75] Grebenkov D S and Tupikina L 2018 Heterogeneous continuous-time random walks *Phys. Rev.* E **97** 012148
[76] Levernier N, Dolgushev M, Bénichou O, Voituriez R and Guérin T 2019 Survival probability of stochastic processes beyond persistence exponents *Nat. Commun.* **10** 2990
[77] Grebenkov D S, Metzler R and Oshanin G 2019 Full distribution of first exit times in the narrow escape problem *New J. Phys.* **21** 122001
[78] Grebenkov D S 2019 A unifying approach to first-passage time distributions in diffusing diffusivity and switching diffusion models *J. Phys. A: Math. Theor.* **52** 174001
[79] Lawley S D 2020 Distribution of extreme first passage times of diffusion *J. Math. Biol.* **80** 2301–25
[80] Bartholomew C H 2001 Mechanisms of catalyst deactivation *Appl. Catal. Gen.* **212** 17–60
[81] Filoche M, Grebenkov D S, Andrade J S Jr and Sapoval B 2008 Passivation of irregular surfaces accessed by diffusion *Proc. Natl Acad. Sci.* **105** 7636–40
[82] Papanicolaou V G 1990 The probabilistic solution of the third boundary value problem for second order elliptic equations *Probab. Theor. Relat. Field* **87** 27–77
[83] Bass R F, Burdzy K and Chen Z-Q 2008 On the Robin problem in fractal domains *Proc. Lond. Math. Soc.* **96** 273–311
[84] Donsker M D and Varadhan S R S 1975 Asymptotic evaluation of certain markov process expectations for large time, II *Commun. Pure Appl. Math.* **28** 279–301
[85] Angeletti F and Touchette H 2016 Diffusions conditioned on occupation measures *J. Math. Phys.* **57** 023303

J. Stat. Mech. (2020) 103205